3-2-2023 9:30 AM

Longitudinal Computed Tomography Airway Measurements in Ex-Smokers with and without Chronic Obstructive Pulmonary Disease

Paulina V. Wyszkiewicz, *The University of Western Ontario*

Supervisor: Parraga, Grace, *The University of Western Ontario*
Co-Supervisor: Cunningham, Ian A., *The University of Western Ontario*
A thesis submitted in partial fulfillment of the requirements for the Master of Science degree in Medical Biophysics

Abstract

Chronic obstructive pulmonary disease (COPD) is a heterogeneous disease characterized by chronic airflow obstruction, emphysematous destruction, and airway remodeling. Thoracic CT has previously revealed abnormalities in the small airways, where disease onset is believed to initiate. In previous COPD cohort studies, airway wall thinning and diminished total airway count (TAC) were observed with increasing disease severity. However, longitudinal insights are lacking. Accordingly, the objective of this thesis was to evaluate longitudinal CT airway measurements at baseline and after three-years in ex-smokers. I observed that CT TAC was decreased only in ex-smokers with COPD, whilst airway walls were thinner in both ex-smokers with and without COPD. To my knowledge, this is the first study to show TAC worsening over time in COPD, which suggests airway narrowing, obstruction, and/or obliteration. These longitudinal three-year findings in ex-smokers, in whom forced expiratory volume in 1-second did not change, provide insights into mechanisms of COPD progression.

Keywords

Chronic obstructive pulmonary disease, ex-smokers, computed tomography, disease progression, small airway abnormalities, longitudinal measurements

Summary for Lay Audience

Chronic obstructive pulmonary disease (COPD) is a debilitating disease that worsens over time and results in symptoms such as chronic cough, difficulty breathing, wheezing, mucus production, and exercise limitation. It is most commonly caused by long-term exposure to tobacco cigarette smoke. COPD is believed to start in the small airways and then progress to other structures in the lungs. Breathing tests performed at the mouth are the current standard for clinical diagnosis and disease management. Unfortunately, these tests only provide global measurements of lung function, cannot inform on the unevenness of how inhaled air spreads throughout the lungs, and cannot capture changes and abnormalities in the small airways. Computed tomography (CT) imaging allows the visualization and evaluation of regional abnormalities in the lungs, including emphysema and airway structure. Importantly, airways on CT may reflect small airway abnormalities and provide additional information beyond what is offered with breathing tests. Previous research studies have shown that with increasing disease severity, the total number of airways on CT decreases and airway walls become thinner in patients with COPD. However, changes in these measurements over time are not well understood. Therefore, the objective of this thesis was to evaluate CT airway measurements in ex-smokers at their first visit and then again after three-years. In these participants, measurements of lung function evaluated with breathing tests did not change or worsen over this time period. I observed that the total number of airways was decreased after three-years only in ex-smokers with COPD, while airway walls were thinner in both ex-smokers with and without COPD. To my knowledge, this is the first study to show longitudinal worsening in the total number of CT-visible airways of patients with COPD. This finding may suggest that airways become thinned, blocked, and/or destroyed over time. Together, these results provide a better understanding of how airway structure changes over time in ex-smokers and patients with COPD. Furthermore, it demonstrates the benefit of using CT imaging to help researchers and clinicians to better evaluate and manage disease progression.

Co-Authorship Statement

This thesis contains one manuscript that has been submitted for publication in a scientific journal. As first author of this manuscript, I significantly contributed to all aspects of the study as well as drafting and completing the final manuscript and its submission. I was also responsible for image processing and statistical analyses and interpretation. Grace Parraga, as the Principal Investigator and thesis Supervisor, provided continued guidance and was responsible for the conception of the study, experimental design, data interpretation, and approval of the final manuscript. She was also the guarantor of the data integrity and responsible for Good Clinical Practice. Patient study visits and acquisition of pulmonary function data were performed under the supervision of Lyndsey Reid-Jones, Rachel Eddy, and Danielle Knipping. Polarization of hyperpolarized gas was performed by Andrew Wheatley, Dante PI Capaldi, Heather Young, and Andrew Wescott. MRI acquisition was performed by Trevor Szekeres and David Reese. Below are the specific contributions for all co-authors for Chapter 2.

Chapter 2 is an original research article entitled "*Reduced Total Airway Count and Airway Wall Tapering after Three-years in Ex-smokers*" and was submitted to the *Journal of Chronic Obstructive Pulmonary Disease* on February 3, 2023. The manuscript was co-authored by Maksym Sharma, Vedanth Desaigoudar, Ian A Cunningham, David G McCormack, Mohamed Abdelrazek, Miranda Kirby, and Grace Parraga. I was responsible for image processing, statistical analyses and interpretation, as well as drafting and completing the final manuscript and its submission. Maksym Sharma and Vedanth Desaigoudar assisted with data analysis and interpretation. David G McCormack was responsible for recruitment of study participants, clinical input in the study design, and clinical interpretation of the data. Ian A Cunningham and Mohamed Abdelrazek assisted with technical and clinical interpretation of the data, respectively. Miranda Kirby assisted with participant recruitment and data acquisition and interpretation. Grace Parraga was responsible for the conception of the study, experimental design, data interpretation, and approval of the final manuscript, as well as being the guarantor of study data integrity. All co-authors had an opportunity to review and revise the manuscript and approved its final submitted version.

Acknowledgments

I would first like to thank my supervisor, Dr. Grace Parraga. The opportunities you have provided me with are incredibly unique; from working on original research articles, review articles, abstracts, and conference presentations, to the opportunity to continually collaborate with colleagues and interact with study participants. These opportunities and experiences have pushed me to grow both personally and professionally, even more than I could have imagined throughout my graduate studies.

I would also like to thank my co-supervisor, Dr. Ian Cunningham, as well as the members of my advisory committee: Dr. Paula Foster and Dr. Mohamed Abdelrazek for your support and guidance. Your though-provoking comments and feedback during committee meetings were immensely helpful in improving my research and preparing me for my thesis dissertation.

A special thank you goes to all the members of the Parraga lab. I feel very lucky to be part of such a collaborative and intelligent group of people that have made my time at Robarts and Western incredibly memorable. To Angela Wilson, I am grateful to be able to call you my friend – a visit to your office always put a smile on my face and I very much enjoyed having a good laugh with you. You always listened when I wanted to talk or needed advice, but I especially thank you for your exceptionally magnificent baking skills. To Kiran Kooner, thank you for being my go to person and great friend – from helping me with Vida to just needing someone to chat and laugh with. You were always so kind to me, I will never forget our fun times together. To Maks Sharma, thank you for showing me the ropes and collaborating with me on the everlasting dataset that is TINCan. You are a caring lab mate and friend. To Marrissa McIntosh, thank you for your great advice and collaboration – you always take the time to answer my questions and help me with projects, abstracts, and presentations. To Alex Matheson, thank you for your support and guidance as the senior member of the lab – your advice was invaluable. To Ivailo Petrov, thank you for showing me the ropes on polarizing and always lending a helping hand for anything and everything, whether that be lab related or not. To Hana Serajeddini, thank you for you clinical input and guidance. You are such a positive and kind person, I really enjoyed our chats in Angela's office.

To the students and personnel at Robarts and Western, thank you for making my graduate experience engaging, thought-provoking, and fun. To Lisa Garland and Victor Chu, I really appreciate your friendship and collaboration – it was amazing to embark on this graduate school journey together. Thank you for providing me with such a positive academic experience and for being my go to buddies for Grad Club lunch.

Finally and most importantly, my sincerest gratitude goes towards my family and friends. To my Mom and Grandma, thank you for always believing in me and supporting me throughout all my endeavors. You are the kindest, most caring, and loving people in the world, I am so thankful to have you in my life. I would especially like to thank my grandma for being like a second mother to me – I will never forget all your hard work and dedication, KCBNZCS. To Luke, thank you for your continuous support and for being a positive light in my life, but especially for always making me laugh and putting a smile on my face. To all my physics friends, Jill, Jenna, Margarita, Nadia, Gabe, and Ridwan, thank you for your support during my undergraduate studies – you all made my experience so fun and memorable.

Table of Contents

List of Tables

List of Figures

List of Appendices

List of Abbreviations

^{3}He	Helium-3
6MWD	Six Minute Walk Distance
BMI	Body Mass Index
COPD	Chronic Obstructive Pulmonary Disease
CT	Computed Tomography
DL_{CO}	Diffusing Capacity of the Lung for Carbon Monoxide
FEV_1	Forced Expiratory Volume in 1 Second
FVC	Forced Vital Capacity
FRC	Functional Residual Capacity
GOLD	Global Initiative for Chronic Obstructive Lung Disease
HU	Hounsfield Units
LA	Lumen Area
MRI	Magnetic Resonance Imaging
RA_{950}	Relative Area of the Lung <-950 HU
RV	Residual Volume
SaO_2	Oxygen Saturation
SGRQ	St. George's Respiratory Questionnaire
TAC	Total Airway Count
TINCan	Thoracic Imaging Network of Canada
TLC	Total Lung Capacity
TV	Tidal Volume
VDP	Ventilation Defect Percent
WA	Wall Area
WA%	Wall Area Percent
WT%	Wall Thickness Percent

CHAPTER 1

1 INTRODUCTION

Chronic obstructive pulmonary disease (COPD) is a progressive disease defined by persistent airflow limitation. Spirometry serves as the gold-standard for clinical evaluation and diagnosis of patients with COPD. However, it only provides global measurements of lung function and is not sensitive to pathophysiological abnormalities, especially in the small airways. Thoracic CT serves as the clinical mainstay for COPD imaging, providing imaging phenotypes of emphysema and small airways disease. In this thesis, airway structure was quantified with CT imaging and evaluated longitudinally to develop a deeper understanding of disease progression in ex-smokers with and without COPD.

1.1 Motivation and Overview

Chronic obstructive pulmonary disease (COPD) is a heterogeneous disease characterized by chronic airflow obstruction,[1] emphysematous destruction, and airway abnormalities.[2] Over 300 million people are affected by COPD worldwide,[3] with approximately 2 million people aged 35 years and older affected in Canada.[4] Individuals living with COPD may experience shortness of breath, chronic cough, exercise limitation, and overall impaired participation in daily life. The primary cause and largest risk factor for COPD is tobacco smoke exposure, as approximately 25% of smokers will develop COPD in their lifetime.[5] Non-smoking individuals can also develop COPD based on a genetic condition such as alpha-1 anti-trypsin deficiency[6] or due to environmental factors[7] and occupational exposures.[8]

In healthy non-smoking individuals, age-related decline in pulmonary function is a normal physiological process, as illustrated in **Figure 1.1**.[9] Non-smokers without respiratory disease almost never develop clinically significant airflow obstruction and their lung function declines steadily with age. Smokers develop different degrees of airflow obstruction depending on their susceptibility to the effects of tobacco exposure. These individuals have an increased rate of pulmonary function decline, which ultimately

becomes disabling or deadly. Fortunately, smoking cessation may make a large difference in the rate of lung function decline of a susceptible smoker.[9]

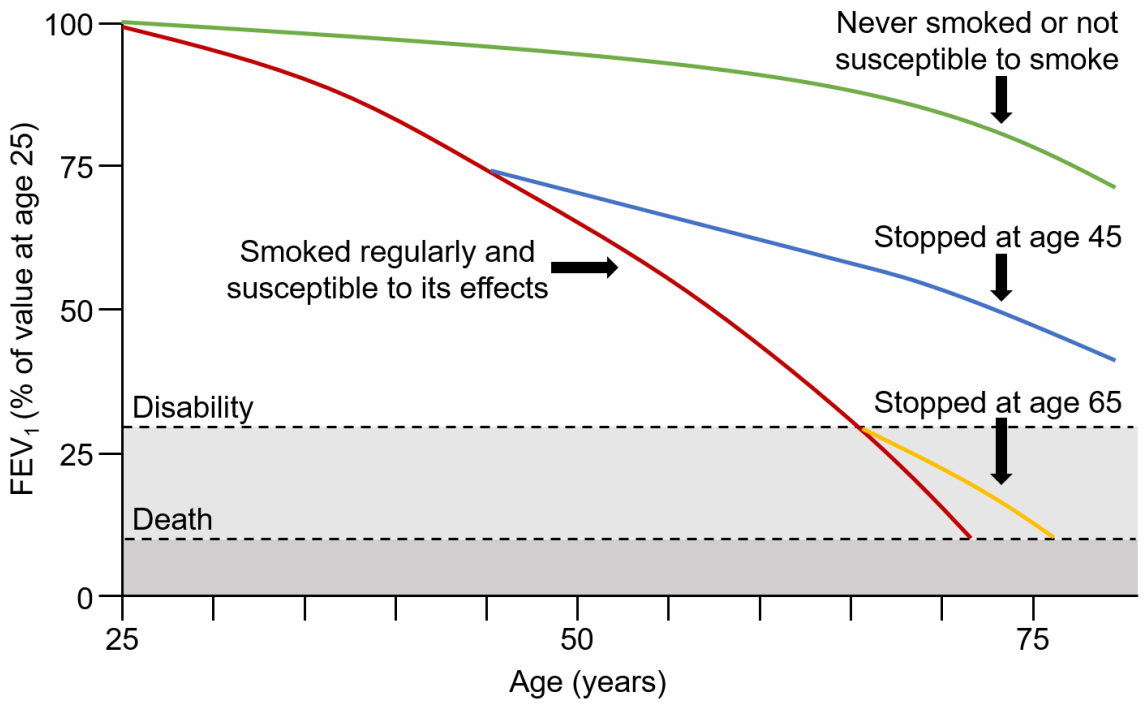

Figure 1.1: Schematic of the natural history of pulmonary function decline in smokers and healthy never-smokers over a lifespan.
This schematic demonstrates the trajectory of normal age-related pulmonary function decline (green), as measured with the forced expiratory volume in 1-second (FEV_1), at the peak age of 25. In individuals who smoke regularly and are susceptible to its effects, smoking-related lung function decline (red) has an accelerated trajectory towards disability and death. In smokers who quit at the age of 45, this decline (blue) can be slowed to resemble a more normal trajectory. In those who quit later at age 65, this decline (yellow) can also be slowed but not to as normal of a trajectory as if one were to quit smoking earlier in life. Adapted from Fletcher and Peto (1977).[9]

COPD diagnosis is considered in patients with symptoms of dyspnea, chronic cough or sputum production, and a history of risk factors, particularly tobacco smoking, according to the Global Initiative for Chronic Obstructive Lung Disease (GOLD) strategy for diagnosis and management criteria.[1] However, spirometry is required to confirm the presence of persistent airflow limitation for COPD diagnosis. These tests are relatively simple and inexpensive; however, they only provide global measures of lung function and do not encapsulate the complex heterogeneity of the disease. Patients with COPD often

experience worsening symptoms over time, which can lead to exacerbations and become life-threatening. Therefore, the evaluation and management of disease progression is critical in these patients and in those at risk of developing COPD.

In this Chapter, the pertinent background information is provided to motivate the original research presented in **Chapter 2**. An overview of the structure and function of the lungs is described (**1.2**), followed by the pathophysiology of COPD (**1.3**). Latterly, clinical tools and measures of pulmonary function are provided (**1.4**), as well as clinical assessments to characterize COPD (**1.5**). Furthermore, the current techniques and biomarkers for imaging pulmonary structure and function are detailed (**1.6**). Cross-sectional evaluations in COPD which have laid the ground work and served as motivation for the original work presented in this thesis are subsequently described (**1.7**). Finally, the specific hypotheses and objectives for this original work are introduced (**1.8**).

1.2 Pulmonary Structure and Function

The respiratory system consists of airspaces including the airways and alveoli, as well as lung parenchyma. The primary function of the lung is to perform gas exchange, allowing oxygen from inhaled air to enter the bloodstream, and for carbon dioxide to exit. In this section, the structure and function of the respiratory system will be described.

1.2.1 Airways

The airways are defined as a series of tubes that continue to branch as they extend deeper into the lung, becoming narrower, shorter, and more numerous.[10] Air is inhaled through the nose or mouth, and then travels down the pharynx, passes through the larynx and into the trachea. The trachea divides into the right and left main bronchi, with one leading to the left lung and the other to the right lung. The bronchi divide into the lobar bronchi, which supply the five lung lobes, including the upper, middle, and lower lobes in the right lung and the upper and lower lobes in the left lung. The lobar bronchi divide into the segmental bronchi, which consist of the 19 anatomically and functionally distinct bronchopulmonary segments, shown in the labeled airway tree in **Figure 1.2**. The airways continue to branch down to the smallest airways without alveoli, called the terminal bronchioles. All of these airways, from the trachea (generation 0) to the terminal bronchioles (generation 16), make

up the conducting zone, shown in **Figure 1.2**, which acts as a conduit to lead inhaled air to the respiratory zone where gas exchange occurs. The conducting airways do not take part in gas exchange as they do not contain alveoli, and thus are known as the anatomic dead space with an approximate volume of 150 mL.[10]

The terminal bronchioles divide into the respiratory bronchioles, which start to contain alveoli. The respiratory bronchioles then divide into the remaining distal airways up to the alveolar ducts, and finally the alveolar sacs, which are completely lined with alveoli. All of these airways, from the respiratory bronchioles (generation 17) to the alveolar sacs (generation 23), make up the respiratory zone, shown in **Figure 1.2**. While the larger proximal airways are composed of mostly cartilage, as the airways branch distally the proportion of cartilage decreases and smooth muscle increases, such that the distal airways are composed of mostly smooth muscle.

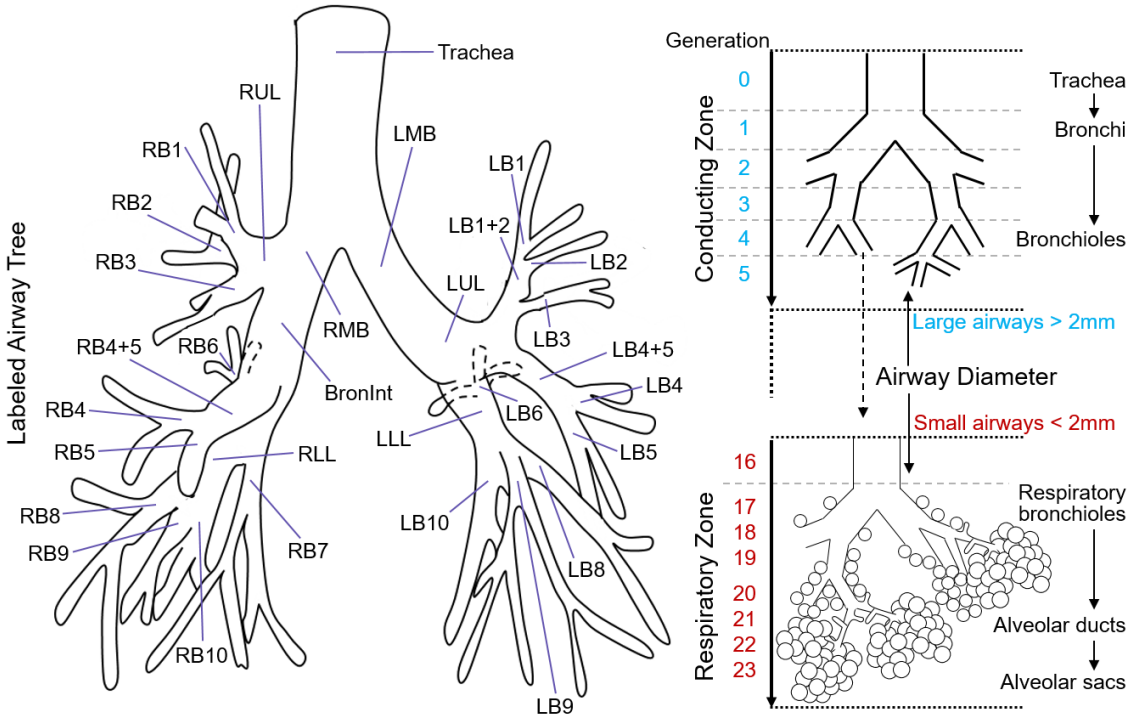

Figure 1.2: Schematic of airway tree structure.
This schematic illustrates the airway tree (left) with segmental labels. Adapted from Tschirren et al. (2006).[11] The human airway tree consists of the conducting zone; generations 0 to 16, and the respiratory zone; generations 17 to 23 (right). Adapted from West's Respiratory Physiology: The Essentials 11th edition[10] and Sharma et al. (2022).[12]

1.2.2 Parenchyma

The lung parenchyma is comprised of about 500 million alveoli, each with a diameter of approximately 300 μm, and is the site involved in gas exchange.[10] Each alveolus is surrounded by a network of capillaries that create the blood-gas interface. Oxygen and carbon dioxide move across the blood-gas interface according to Fick's law of diffusion, which states that the amount of gas diffusing is proportional to the area of the interface, but inversely proportional to its thickness. The blood-gas interface is very thin and has a large alveolar surface area of 50 to 100 m^2, therefore the lung is well suited for gas exchange, as shown in **Figure 1.3**. Inhaled air enters the lungs, travels through the large and small airways to the alveoli, diffuses across the alveolar-capillary interface into the bloodstream, and binds to red blood cells. Carbon dioxide from the bloodstream diffuses into the alveolus and is exhaled.

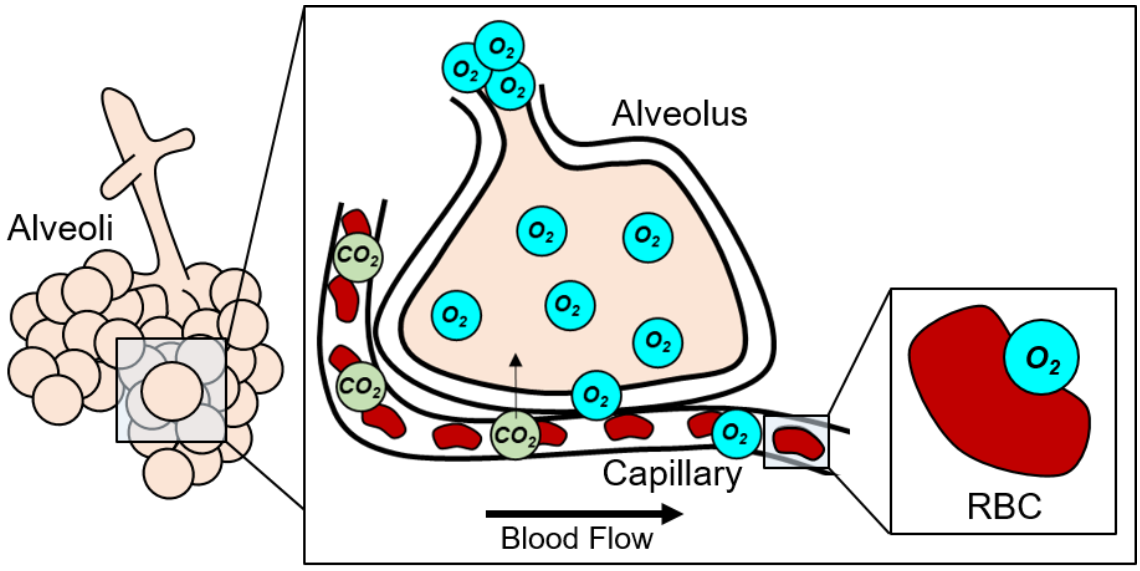

Figure 1.3: Diagram of gas exchange from the alveoli into the bloodstream.
This figure illustrates oxygen (O_2) (cyan) from the alveolus, diffusing across the capillary membrane into the bloodstream to bind with red blood cells (RBC) (red). Carbon dioxide (CO_2) (green) diffuses from the bloodstream to the alveolus and is removed upon exhalation. Adapted from Sharma et al. (2022).[12]

1.3 Pathophysiology of Chronic Obstructive Pulmonary Disease

The structure, consisting of the airways and parenchyma, and the function of the lungs, consisting of gas exchange, were described above. Abnormalities in these structures will impact gas exchange within the lung, resulting in obstructive lung disease. The defining characteristic of COPD is irreversible airflow limitation,[1] caused by lesions that obstruct the small conducting airways,[13,14] produce parenchymal lung damage,[15] or both, as shown in **Figure 1.4**. In this section, the underlying known pathophysiologies of the respiratory system in COPD are presented.

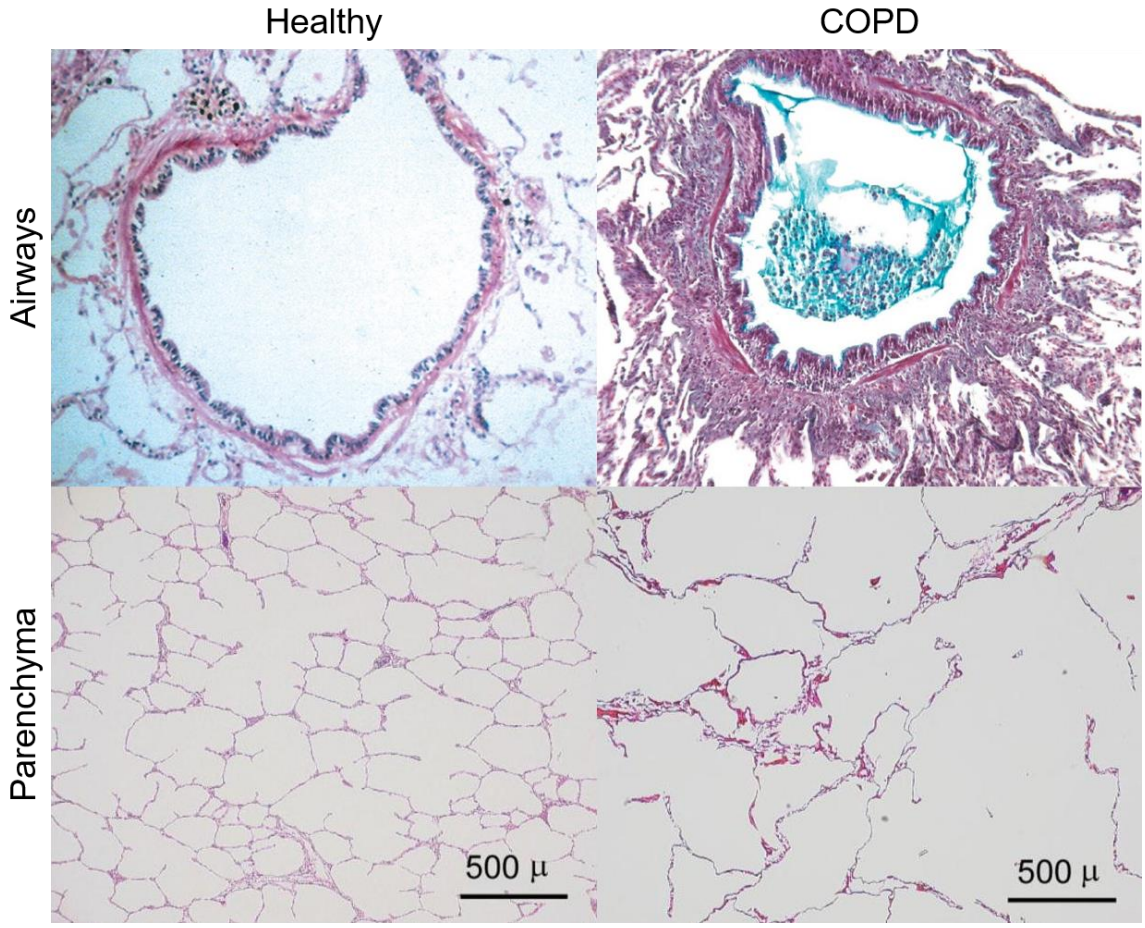

Figure 1.4: Diagram of airway and parenchymal pathophysiology in COPD.
This diagram shows airway histology from a healthy and diseased lung (top). Adapted from Hogg (2004).[16] Parenchyma histology from a healthy and diseased lung (bottom) are also shown. Adapted from Woods et al. (2006).[17]
Permissions to reproduce all images are provided in Appendix B.

1.3.1 Small Airways Disease

The major site of airway obstruction and structural airway remodeling in COPD is found in the small conducting airways, which are less than 2 mm in diameter (generations 4-16).[13] Due to chronic inflammation, the accumulation of mucus obstructs the small airways of patients with COPD, resulting in airway wall thickening, as shown in **Figure 1.4**.[16] Previous work has shown that the accumulation of inflammatory exudates containing mucus in the airway lumen of surgically resected lung tissue are related to COPD severity.[18] The increase in tissue between the airway smooth muscle and the lumen surface increases small airway resistance to airflow.[16] Studies have shown connective tissue deposition in the adventitial compartment of the airway wall in advanced emphysema,[19] causing fixed airway obstruction through the restriction of airway caliber enlargement during lung inflation.[18] This inflammatory process may also destroy alveolar support to the small airways; however, direct measurements of peripheral airway resistance indicate that the loss of this support is less important to disease severity as compared to airway wall and lumen pathology.[13]

1.3.2 Emphysema

Emphysema, also known as parenchymal lung destruction, is defined by dilatation and destruction of lung tissue beyond the terminal bronchiole.[20] In patients with COPD, airflow limitation is associated with emphysematous destruction, which reduces the lung's elastic recoil force.[15] This loss in elasticity results in hyper-inflated lungs since they are unable to completely empty. Pulmonary emphysema, shown in **Figure 1.4**, is divided into three main subtypes: centrilobular, panlobular, and paraseptal emphysema.[21] Centrilobular emphysema, which is most closely associated with tobacco smoking, results from dilatation and destruction of the respiratory bronchioles while preserving the alveolar ducts and sacs, and is most common in the upper lobes of the lung.[16] It usually dominates in advanced disease and is associated with more severe small airway obstruction.[17] Panlobular emphysema, which is closely associated with alpha-1 anti-trypsin deficiency, causes a more even dilation and destruction over the entire acinus and is commonly found in the lower lobes.[16] Paraseptal emphysema results from the destruction of the outer part of the lobule near the septa.[16] Previous work has shown an association of centrilobular and

panlobular emphysema with increased symptoms and reduced exercise capacity independent of airflow obstruction, whilst paraseptal emphysema showed little physiologic significance.[21]

1.4 Clinical Measures of Pulmonary Function

Pulmonary function tests provide objective measurements of global lung function and play an important role in the diagnosis and management of patients with COPD. These clinical tools are simple and cost-effective, while providing information on different aspects of the disease. In this section, pulmonary function tests relevant to the original work presented in this thesis are introduced.

1.4.1 Spirometry

Spirometry measures the amount of air an individual inhales or exhales as a function of time and is the most common pulmonary function test.[22] The most important measurements of the test for clinical COPD diagnosis are the forced expiratory volume in one second (FEV_1) and the forced vital capacity (FVC). FEV_1 describes the total volume of air exhaled in the first second of forced expiration, while FVC represents the total volume of air that is forcibly exhaled.[22] When dividing these two measurements, the FEV_1/FVC ratio provides a measure of airflow obstruction. FEV_1 and FVC are measured in units of volume and are commonly reported as the percent of a predicted value ($\%_{pred}$) using reference equations based on the patient's age, height, sex, and ethnicity.[23] **Figure 1.6** illustrates a spirometer and a corresponding volume-time curve. Spirometry is used to diagnose patients with COPD, as well as to determine disease severity, which will be discussed in more detail in the next section.

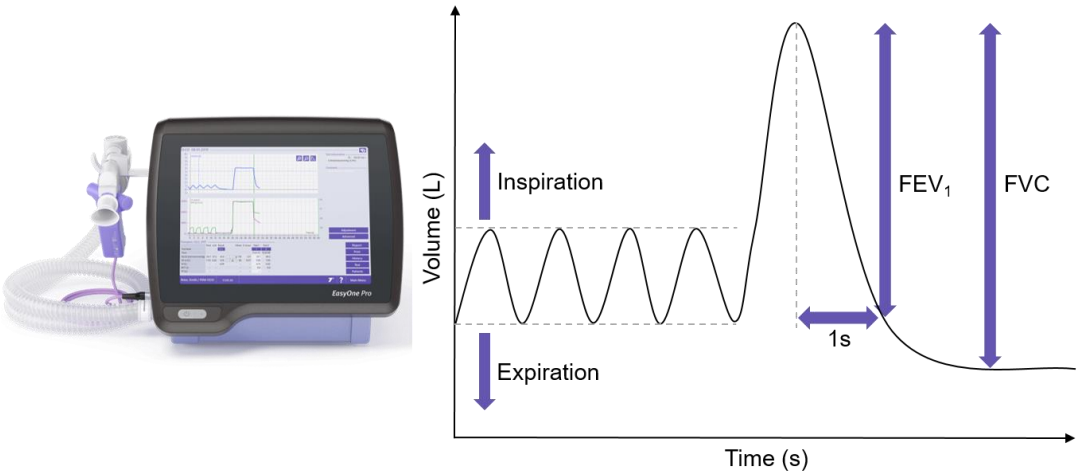

Figure 1.5: Spirometer and typical volume-time curve.
Spirometer records volume-time curve to measure forced expiratory volume in 1-second (FEV_1) and forced vital capacity (FVC).

1.4.2 Plethysmography

Whole body plethysmography measures lung volumes and capacities by analyzing volume changes in the body.[24] **Figure 1.7** illustrates a whole-body plethysmograph and a corresponding volume-time curve displaying the measured lung volumes and capacities. Tidal volume (V_T) represents the volume of air inhaled or exhaled during a standard respiratory cycle, also known as tidal breathing. Functional residual capacity (FRC) describes the volume of air present in the lungs at end-expiration during tidal breathing. Residual volume (RV) represents the volume of air remaining in the lungs after full exhalation. Vital capacity (VC) refers to the volume of air that can be inhaled from full expiration. Total lung capacity (TLC) describes the total volume of air in the lungs which is measured at full inspiration. Similar to spirometry, lung volumes and capacities can be expressed as a $\%_{pred}$ value based on the patient's age, height, sex, and ethnicity.[25] By measuring the pressure and volume in the box and at the mouth, before and after inspiration, the whole body plethysmograph is able to measure lung volumes using Boyle's law, which relates pressure and volume in an isothermal environment.[10]

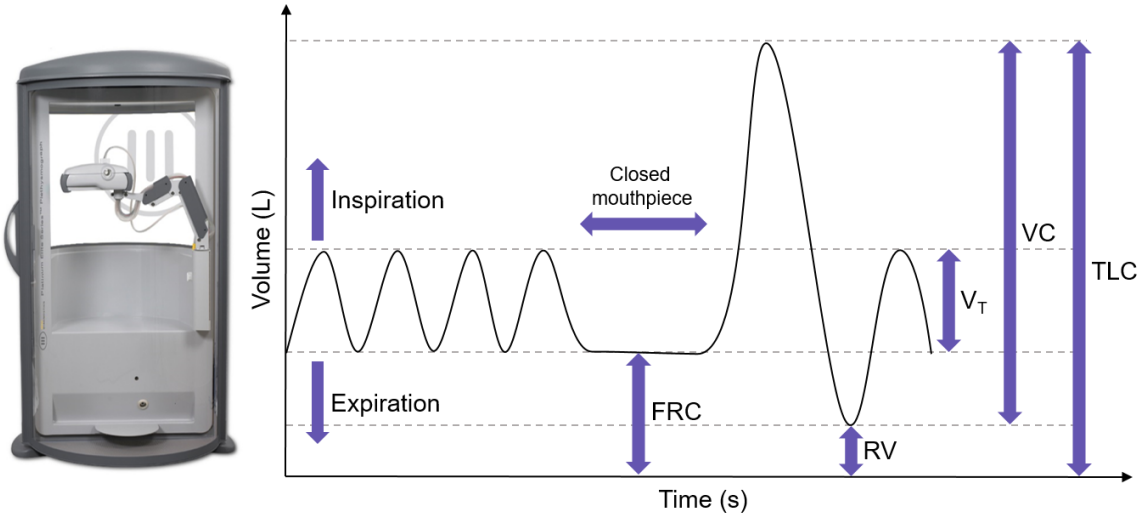

Figure 1.6: Whole-body plethysmograph and typical volume-time curve.
Whole-body plethysmograph measures lung volumes and capacities.
FRC=functional residual capacity; RV=residual volume; TLC=total lung capacity; VC=vital capacity; V_T=tidal volume.

Plethysmography is helpful for detecting, characterizing, and quantifying the severity of lung disease.[24] Air trapping is often expressed as the ratio of RV to TLC (RV/TLC).[26] In patients with COPD, air trapping is caused by an increase in RV due to small airway inflammation and obstruction, as well as emphysematous tissue destruction.

1.4.3 Diffusing Capacity of the Lung

The diffusing capacity of the lung for carbon monoxide (DL_{CO}) measures the ability of the lungs to exchange gas across the alveolar-capillary interface and is commonly performed using the single-breath technique.[27] Carbon monoxide is used to measure gas exchange within the lungs since it has a high affinity for hemoglobin and follows the same path as oxygen to bind with hemoglobin.[28] DL_{CO} is dependent on many structural and functional properties in the lungs and can be used to assess the severity of obstructive and restrictive lung diseases, as well as pulmonary vascular diseases. In patients with COPD, DL_{CO} may be decreased due to emphysematous alveolar destruction by reducing the surface area available for gas exchange.

1.5 Clinical Assessments to Characterize COPD

Pulmonary function tests outlined above, particularly spirometry, are used for COPD diagnosis and assessment of disease severity. Validated questionnaires have been developed to evaluate patient-reported outcomes, while exercise capacity tests provide a way to objectively assess functional capacity in patients with COPD.

1.5.1 Disease Severity

COPD severity is classified according to the Global Initiative for Chronic Obstructive Lung Disease (GOLD) guidelines, using spirometry thresholds.[1] The diagnosis of COPD is confirmed by post-bronchodilator spirometry when the FEV_1/FVC ratio is less than 0.7. Airflow limitation severity is then assessed with the post-bronchodilator value of FEV_1 $\%_{pred}$. **Table 1.1** shows the FEV_1 thresholds that define each level of COPD severity, from mild (GOLD I) to very severe (GOLD IV).

Table 1.1: Diagnostic cut-offs for COPD severity classification according to GOLD criteria.

In patients with $FEV_1/FVC < 0.70$		
Grade	**Severity**	**FEV_1 ($\%_{pred}$)**
GOLD I	Mild	$\geq 80\%$
GOLD II	Moderate	$\geq 50\%$, $< 80\ \%$
GOLD III	Severe	$\geq 30\%$, $< 50\%$
GOLD IV	Very Severe	$< 30\%$

Adapted from the 2022 GOLD Report.[1]

Although spirometry remains the clinical gold standard for COPD diagnosis and management, it does not inform on the heterogeneity of the disease and cannot differentiate the relative causes of obstruction, airway inflammation, emphysema, or small airway abnormalities.[29] Spirometry alone is insufficient in effectively assessing this heterogeneous disease, therefore other measurements are required for better COPD phenotyping. In the next section, thoracic imaging techniques will be discussed in order to address these limitations.

1.5.2 Questionnaires

Quality of life questionnaires are important clinical tools to investigate disease burden in COPD, by evaluating a patient's perception of their respiratory disease. The St. George's Respiratory Questionnaire (SGRQ) is a standardized self-completed measure of quality of life and is most commonly used in patients with COPD.[30] It measures the impact of chronic airflow limitation on an individual's overall health, daily activities, and perceived well-being. The SGRQ consists of 76 items and is partitioned into three-sections; symptoms, activity, and impacts, such that each section is scored separately from 0 to 100, zero indicating no impairment. A summary of the responses from all sections is used to calculate the total SGRQ score. The minimum clinically important difference for the SGRQ score in patients with COPD is 4 units.[31]

1.5.3 Exercise Capacity Tests

Exercise capacity tests provide more objective measurements of an individual's true functional capacity, which may be overestimated or underestimated when using self-reported measurements. Walk tests are often used as measures of functional exercise tolerance in patients with exercise limitations due to COPD. The six-minute walk test (6MWT) is a simple measure of sub-maximal exercise capacity, where the patient walks at their usual pace for six-minutes.[32] Other exercise capacity tests exist; however, the 6MWT is easier to administer, better tolerated, better reflects activities of daily living, and has been used in clinical settings.[33] The measured outcome of this test is the six-minute walk distance (6MWD), which strongly correlates with FEV_1[34] and is an independent predictor of mortality in COPD.[35] A clinically important change in 6MWD is 70 m in patients with COPD.[33]

1.6 Imaging of Pulmonary Structure and Function

In section 1.4, pulmonary function tests were presented as simple, inexpensive methods to measure global lung function in respiratory diseases including COPD. In section 1.5, questionnaires and exercise capacity tests were presented as additional tools to evaluate disease burden and pulmonary functional capacity. Unfortunately, these measurements cannot inform on the regional heterogeneity of the disease, cannot estimate regional small

airway and parenchymal abnormalities,[2,13] and are weakly predictive of early disease and disease progression. Pulmonary imaging however, provides the opportunity to visualize and quantitatively analyze regional structural and functional information in the lungs. In this section, pulmonary imaging modalities relevant to the original work presented in this thesis are introduced.

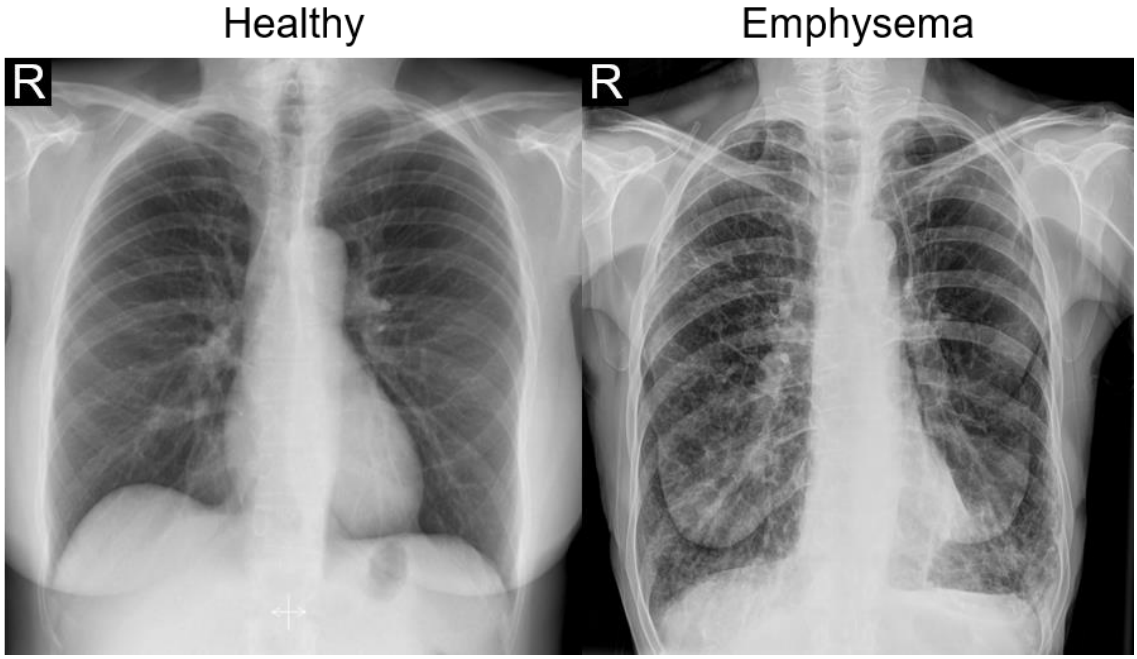

Figure 1.7: Chest x-ray in a healthy participant and in a COPD patient with emphysema.
Healthy: Case courtesy of Usman Bashir, Radiopaedia.org, rID: 18394
Emphysema: Case courtesy of Ian Bickle, Radiopaedia.org, rID: 50326

1.6.1 Planar X-ray

Planar x-ray is the most frequently performed imaging modality to image the chest and lung disease, shown in **Figure 1.7**. An x-ray beam is produced at the radiation source and traverses the patient to the detector plate generating a two-dimensional image. X-ray imaging provides good image contrast for distinguishing high-attenuating structures, such as bone, from low-attenuating structures, such as lung parenchyma. Chest x-rays are simple, relatively inexpensive, and have a low radiation dose; however, they do not provide three-dimensional information and typically require the presence of quite severe lung abnormalities in order to be detected.

1.6.2 Computed Tomography

Computed tomography (CT) is an imaging modality that uses x-rays to generate a three-dimensional image of the body. A narrow beam of x-rays is aimed at a patient and quickly rotated around the body to create cross-sectional images, also known as slices, which are digitally stacked together to form the three-dimensional image. Each voxel of a reconstructed CT image is represented by a measurement of tissue density known as Hounsfield Units (HU) and corresponds to the attenuation of x-rays in the body referenced to attenuation of radiation in water. Air is characterized by HU of -1000, low-attenuating structures such as the lung parenchyma have HU near -800, and high-attenuating structures such as bone have HU near +1000. Thoracic CT serves as the gold-standard imaging approach for COPD by providing high-resolution structural information regarding airways disease[36] and terminal airspace enlargement or emphysema.[37] **Figure 1.8** shows inspiratory CT images in the coronal plane including regions with emphysema present, as well as segmented airway tree images for comparison between ex-smokers without COPD, with mild COPD (GOLD I), moderate COPD (GOLD II), and severe COPD (GOLD III). Through the application of computational analysis, CT imaging biomarkers have been developed to quantitatively evaluate respiratory diseases.[38] Multiple quantitative CT analysis software platforms are commercially available, including VIDAvision from VIDA Diagnostics Inc. (Coralville, IA, USA) which has been approved for clinical use.

An important consideration for CT imaging is the associated dose from ionizing radiation. High-resolution CT images in this thesis were acquired according to a low-dose protocol with an estimated total effective dose of 1.8 mSv.[39] The equivalent risks of the CT examination for an adult is about half a year of natural background radiation,[40] smoking 23 cigarettes,[41] and much less than the risk of being struck by lightning in a lifetime.

Figure 1.8: CT imaging for representative ex-smokers with and without COPD.
The reconstructed CT images (left column) and emphysema maps with RA_{950} threshold in yellow (middle column) are shown. The three-dimensional reconstructions of the segmented airway trees (right column) are also shown.
Ex-smoker: 70 year old female, FEV_1 = 93%$_{pred}$, FEV_1/FVC = 85%, RA_{950} = 1%, TAC = 306. Mild COPD (GOLD I): 75 year old male, FEV_1 = 92%$_{pred}$, FEV_1/FVC = 68%, RA_{950} = 7%, TAC = 265. Moderate COPD (GOLD II): 83 year old male, FEV_1 = 57%$_{pred}$, FEV_1/FVC = 57%, RA_{950} = 20%, TAC = 258. Severe COPD: 67 year old female, FEV_1=37%$_{pred}$, FEV_1/FVC = 31%, RA_{950}=33%, TAC=206.

Airways

Semi- and fully-automated algorithms have been developed to segment the large airways and extract quantitative CT airway measurements. These techniques take advantage of the cylindrical shape of the airways and the inherent contrast between air within the airway lumen and the highly vascularized airway wall. In **Figure 1.8**, CT segmented airway trees are shown and the number of airways are visibly diminished in participants with increasing COPD severity. The total number of CT-visible airways is described by the total airway count (TAC) and was shown to be associated with the number of terminal bronchioles in excised lung specimens measured with micro-CT.[42] Airway wall dimension measurements can also be measured, such as airway wall area (WA), lumen area (LA), wall area percent (WA%), wall thickness (WT), and wall thickness percent (WT%). In COPD, the evaluation of the airways have provided insights into understanding structural abnormalities of the small airways. Previous cross-sectional evaluations investigating these CT airway measurements in COPD will be discussed in the next section, providing additional background and reasoning for the original work presented in this thesis.

Abnormalities in the small airways can also be inferred from air trapping measured on expiratory CT. Air trapping can be quantified using the relative area of the lung with attenuation less than -856 HU.[43] This is the attenuation value of a normally inflated lung, therefore lungs at end expiration should have higher attenuation than -856 HU since they contain less air. CT air trapping has been shown to highly correlate with FEV_1 and FEV_1/FVC in cigarette smokers,[44] as well as progress over five years.[45] A challenge in evaluating expiratory CT air trapping in COPD is that it can be difficult to distinguish between air trapping due to emphysema and small airway disease using a simple threshold.[43] Thus, paired inspiratory and expiratory CT are commonly assessed in COPD and studies have shown that air trapping closely correlates with airway dysfunction regardless of the degree of emphysema.[46]

Parenchyma

CT is ideal for detecting and characterizing emphysema, as well as quantifying its extent. Computer-automated programs have been developed to measure computed lung density

and has removed the subjectivity of reader scoring methods. Emphysematous destruction causes the normal lung to be replaced with air-containing spaces with attenuation values close to -1000 HU.[43] The relative area of the lung with attenuation less than -950 HU (RA_{950}) on inspiratory CT is a validated method to quantify macroscopic emphysema.[47] Several thresholds exist; however, -950 HU is most commonly used. Emphysema is considered present when RA_{950} is greater than 6.8%.[37] CT emphysema has been shown to correlate with FEV_1,[36] DL_{CO},[48] SGRQ scores,[49] and the frequency of exacerbations,[50] as well as to progress over five years.[45] In **Figure 1.8**, the RA_{950} threshold for emphysema is shown in yellow and larger regions of emphysema are evident as disease severity increases.

1.6.3 Magnetic Resonance Imaging

Magnetic resonance imaging (MRI) is a non-invasive, radiation-free imaging modality that uses magnetic fields and radiofrequency waves to generate three-dimensional anatomical images of the body. Powerful magnets create strong magnetic fields which excite and detect the change in the direction of rotational axis of protons found in the water in human tissue. Conventional proton (^{1}H) MRI leverages the nuclear spins of these protons and forces them to align with the magnetic field, providing excellent soft tissue contrast. Hyperpolarized gas MRI employs the inhalation of noble gases, as well as specialized multi-nuclear hardware and pulse sequences to evaluate regional lung structure and function in patients with respiratory disease.

Conventional ^{1}H MRI

Conventional ^{1}H MRI of the lungs is challenging due to the inherent properties of the lung, including air tissue-interfaces and low tissue density, contributing to very low ^{1}H signal intensity. As a result, acquiring sufficient signal to generate adequate contrast within the lungs using conventional methods is difficult. ^{1}H MRI does provide detailed images of structures surrounding the lungs and within the chest cavity, including the mediastinum, chest wall, pleura, heart, and vessels. Therefore it is often acquired in conjunction with pulmonary functional MRI techniques, in order to provide matched anatomical information. Conventional ^{1}H images are shown in **Figure 1.9**, demonstrating low signal within the lung compared to other structures.

Hyperpolarized Gas MRI

Hyperpolarized helium-3 (^{3}He) and xenon-129 (^{129}Xe) MRI provide enhanced contrast mechanisms to measure pulmonary ventilation, microstructure, and gas exchange within the lungs. ^{3}He and ^{129}Xe are stable isotopes that can be hyperpolarized to increase magnetization, thus increasing the signal intensity within the lungs during a breath-hold maneuver.[51] Previously, ^{3}He ventilation image quality has been superior to ^{129}Xe due to the significantly larger polarization with hyperpolarized ^{3}He. However, the scarcity and price increase of ^{3}He gas has caused a transition to the naturally available and cheaper ^{129}Xe gas. In addition, technological advances have yielded ^{129}Xe ventilation images with comparable image quality to that of ^{3}He.[52] Hyperpolarized ^{3}He images are shown in **Figure 1.9**, demonstrating high signal within the lung, as compared to conventional ^{1}H MRI. Ventilation abnormalities were initially quantified using visual scoring[53] and manual segmentation[54,55]; however, semi-automated[52,56-58] and automated[59-62] methods have been developed and are now widely used. The ventilation defect percent (VDP) is the most commonly used MRI metric to quantify ventilation and is calculated as the ventilation defect volume normalized to the thoracic cavity volume.[52] In patients with COPD, VDP is related to spirometry and disease severity,[63] exercise limitation and symptoms,[64] and has been observed to worsen over time.[65] The minimal clinically important difference for ^{3}He MRI VDP is 2%.[66]

Hyperpolarized gases are also widely used for diffusion-weighted MRI, which has been extensively validated.[67,68] Due to the random Brownian motion of ^{3}He and ^{129}Xe, the gas molecules are highly excitable by a magnetic field and undergo self-diffusion, providing excellent MRI contrast. The diffusive movement of these gas molecules will be restricted by the alveolar boundaries in the lung and can be measured with the apparent diffusion coefficient (ADC). A high value for ADC is indicative of alveolar enlargement and/or destruction, which is an early sign of pulmonary emphysema[69] that has been validated with histology.[17] In patients with COPD, ADC is elevated relative to healthy controls and relates to CT emphysema,[63] as expected, and is also related to airflow obstruction,[70,71] and DL_{CO}.[72] ADC measurements are however limited to regions that ventilate during a single breath-

hold of gas, as shown in **Figure 1.9**. Therefore, we are unable to investigate the terminal airspace enlargement in these unventilated regions, which may be the most diseased.

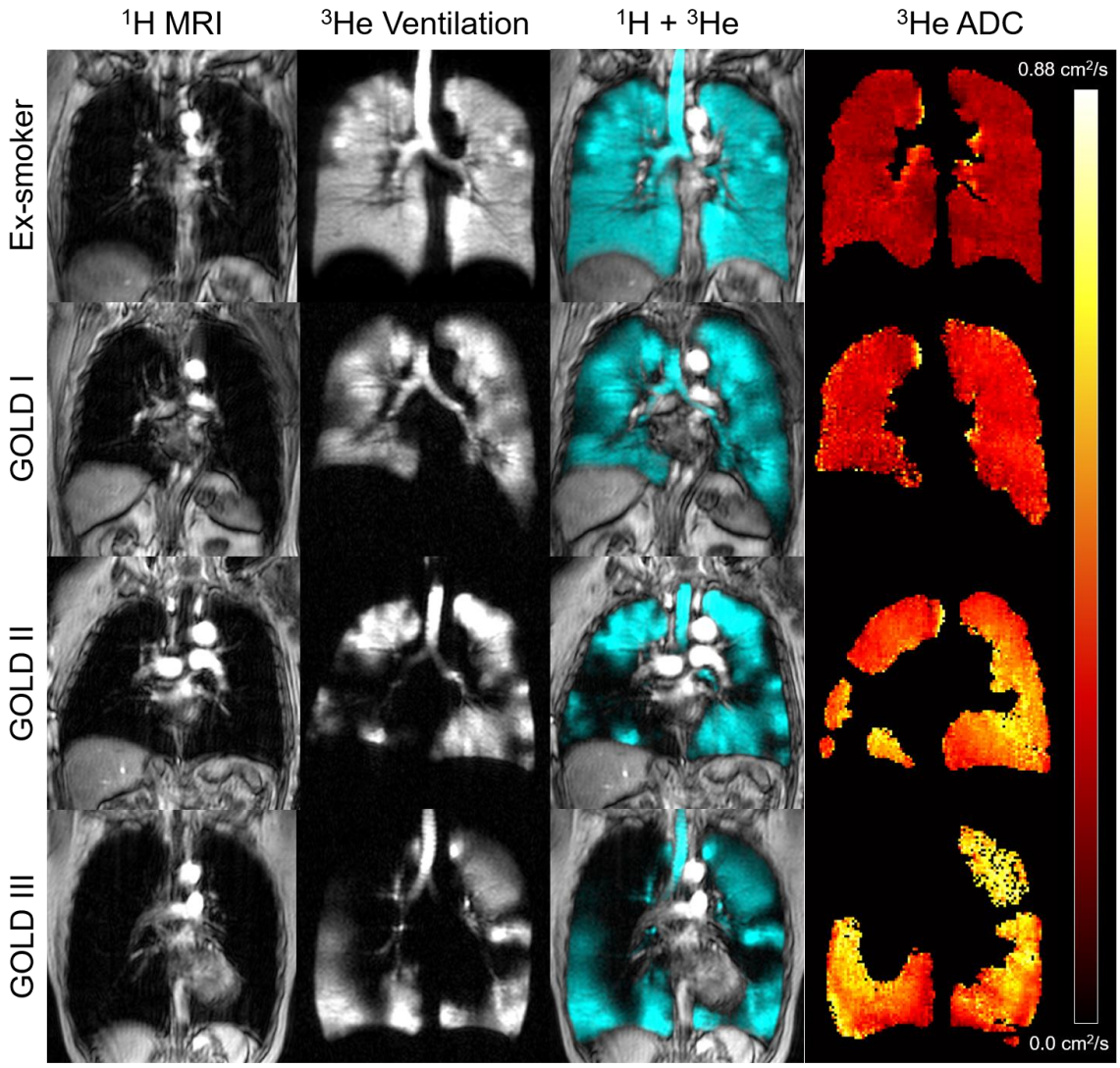

Figure 1.9: Conventional ^{1}H and hyperpolarized ^{3}He MRI for representative ex-smokers with and without COPD.

The conventional ^{1}H (first column), hyperpolarized ^{3}He ventilation (second column) images, and co-registered ^{1}H and ^{3}He (third column) images are shown. The ADC maps reconstructed from the hyperpolarized ^{3}He diffusion-weighted MRI (fourth row) are also shown.

Ex-smoker: 70 year old female, FEV_1 = 93%$_{pred}$, FEV_1/FVC = 85%, VDP = 2%, ADC = 0.23cm^2/s. Mild COPD (GOLD I): 87 year old male, FEV_1 = 92%$_{pred}$, FEV_1/FVC = 68%, VDP = 10%, ADC = 0.31cm^2/s. Moderate COPD (GOLD II): 83 year old male, FEV_1 = 57%$_{pred}$, FEV_1/FVC = 57%, VDP = 24%, ADC = 0.48cm^2/s. Severe COPD: 67 year old female, FEV_1=37%$_{pred}$, FEV_1/FVC = 31%, VDP = 34%, ADC = 0.51cm^2/s.

1.7 Cross-sectional Evaluations in COPD

In previous sections, we discussed the structure and function of the lungs and the pathophysiology of COPD. We introduced clinical tools and measurements used to assess and characterize this disease. Finally, we described imaging techniques to evaluate lung structure and function, and their applications in COPD. In this section, important studies and cross-sectional evaluations in COPD, which have laid the ground work and provided motivation for the original work presented in this thesis, will be introduced.

The onset and progression of COPD are hypothesized to initiate in the small airways; however, the gold-standard of spirometry for COPD diagnosis and management cannot estimate these regional airway abnormalities.[13] Fortunately, thoracic CT provides a way to segment the airway tree and quantify TAC, as well as airway wall dimensions. Although these measurements are limited to the spatial resolution of the CT system, airways visible on CT may reflect histologic small airway dimensions[73] and relate to respiratory symptoms beyond the information offered by spirometry.[74] In previous cross-sectional evaluations, TAC was observed to be diminished with increasing COPD grade severity,[75] was associated with the number of micro-CT terminal bronchioles in excised lung specimens,[42] and was predictive of incident COPD in at-risk ever-smokers.[76] Airway wall thinning was also observed across COPD grade severity[77] and was spatially related to missing airways.[75] These cross-sectional findings provide an understanding of the differences in patients with varying COPD severities; however, it is still unclear how these CT airway measurements change over time, which may provide additional insights into mechanisms of COPD progression.

1.8 Thesis Objectives and Hypotheses

COPD is a debilitating, heterogeneous disease characterized by chronic airflow obstruction,[1] emphysematous lung destruction, and small airway abnormalities.[2] Patients with COPD experience symptoms such as chronic cough, difficulty breathing, wheezing, mucus production, and exercise limitation, which worsen over time. Although spirometry is used for clinical diagnosis and assessment, recent work has shown the potential for quantitative CT airway structure as a biomarker of disease severity and progression.[42,75,76]

To our knowledge, the longitudinal change in the total number of CT-visible airways is yet to be evaluated in COPD.

The overarching objective of this thesis is to investigate longitudinal CT airway abnormalities over three-years in ex-smokers with and without COPD. Specifically, we aim:

1) To evaluate and compare CT airway measurements in ex-smokers with and without COPD at baseline and after three-years,

2) To evaluate relationships between CT airway measurements with MRI ventilation and pulmonary function measurements in ex-smokers, and

3) To investigate imaging and clinical measurements that inform on TAC worsening using prediction models in ex-smokers.

We hypothesized that CT airway measurements would be significantly different after three-years as compared to baseline, in all ex-smokers.

In **Chapter 3**, I provide a summary of the original work presented in **Chapter 2**, followed by the limitations and future directions to build upon the research presented in this thesis. Finally, I conclude with a discussion of the significance and impact of this work.

1.9 Reference

1. Global Initiative for Chronic Obstructive Lung Disease (GOLD). Global Strategy for the Diagnosis, Mangement and Prevention of Chronic Obstructive Pulmonary Disease: 2022 Report. 2021.

2. McDonough JE, Yuan R, Suzuki M, et al. Small-airway obstruction and emphysema in chronic obstructive pulmonary disease. *N Engl J Med.* 2011;365(17):1567-1575.

3. Adeloye D, Song P, Zhu Y, Campbell H, Sheikh A, Rudan I. Global, regional, and national prevalence of, and risk factors for, chronic obstructive pulmonary disease (COPD) in 2019: a systematic review and modelling analysis. *Lancet Respir Med.* 2022;10(5):447-458.

4. Public Health Agency of Canada (PHAC). Report from the Canadian Chronic Disease Surveillance System: Asthma and Chronic Obstructive Pulmonary Disease (COPD) in Canada. 2018.

5. Løkke A, Lange P, Scharling H, Fabricius P, Vestbo J. Developing COPD: a 25 year follow up study of the general population. *Thorax.* 2006;61(11):935-939.

6. American Thoracic Society/European Respiratory Society statement: standards for the diagnosis and management of individuals with alpha-1 antitrypsin deficiency. *Am J Respir Crit Care Med.* 2003;168(7):818-900.

7. Gan WQ, FitzGerald JM, Carlsten C, Sadatsafavi M, Brauer M. Associations of ambient air pollution with chronic obstructive pulmonary disease hospitalization and mortality. *Am J Respir Crit Care Med.* 2013;187(7):721-727.

8. Paulin LM, Diette GB, Blanc PD, et al. Occupational exposures are associated with worse morbidity in patients with chronic obstructive pulmonary disease. *Am J Respir Crit Care Med.* 2015;191(5):557-565.

9. Fletcher C, Peto R. The natural history of chronic airflow obstruction. *Br Med J.* 1977;1(6077):1645-1648.

10. West JB, Luks AM. *Respiratory Physiology: The Essentials.* 11 ed: Wolters Kluwer; 2021.

11. Tschirren J, McLennan G, Palágyi K, Hoffman EA, Sonka M. Matching and anatomical labeling of human airway tree. *IEEE Trans Med Imaging.* 2005;24(12):1540-1547.

12. Sharma M, Wyszkiewicz PV, Desaigoudar V, Guo F, Capaldi DP, Parraga G. Quantification of pulmonary functional MRI: state-of-the-art and emerging image processing methods and measurements. *Phys Med Biol.* 2022;67(22).

13. Hogg JC, Macklem PT, Thurlbeck WM. Site and nature of airway obstruction in chronic obstructive lung disease. *N Engl J Med.* 1968;278(25):1355-1360.

14. Yanai M, Sekizawa K, Ohrui T, Sasaki H, Takishima T. Site of airway obstruction in pulmonary disease: direct measurement of intrabronchial pressure. *J Appl Physiol (1985).* 1992;72(3):1016-1023.

15. Mead J, Turner JM, Macklem PT, Little JB. Significance of the relationship between lung recoil and maximum expiratory flow. *J Appl Physiol.* 1967;22(1):95-108.

16. Hogg JC. Pathophysiology of airflow limitation in chronic obstructive pulmonary disease. *Lancet.* 2004;364(9435):709-721.

17. Woods JC, Choong CK, Yablonskiy DA, et al. Hyperpolarized 3He diffusion MRI and histology in pulmonary emphysema. *Magn Reson Med.* 2006;56(6):1293-1300.

18. Hogg JC, Chu F, Utokaparch S, et al. The nature of small-airway obstruction in chronic obstructive pulmonary disease. *N Engl J Med.* 2004;350(26):2645-2653.

19. Matsuba K, Thurlbeck WM. The number and dimensions of small airways in emphysematous lungs. *Am J Pathol.* 1972;67(2):265-275.

20. The definition of emphysema. Report of a National Heart, Lung, and Blood Institute, Division of Lung Diseases workshop. *Am Rev Respir Dis.* 1985;132(1):182-185.

21. Smith BM, Austin JH, Newell JD, Jr., et al. Pulmonary emphysema subtypes on computed tomography: the MESA COPD study. *Am J Med.* 2014;127(1):94.e97-23.

22. Miller MR, Hankinson J, Brusasco V, et al. Standardisation of spirometry. *Eur Respir J.* 2005;26(2):319-338.

23. Hankinson JL, Odencrantz JR, Fedan KB. Spirometric reference values from a sample of the general U.S. population. *Am J Respir Crit Care Med.* 1999;159(1):179-187.

24. Wanger J, Clausen JL, Coates A, et al. Standardisation of the measurement of lung volumes. *Eur Respir J.* 2005;26(3):511-522.

25. Stocks J, Quanjer PH. Reference values for residual volume, functional residual capacity and total lung capacity. ATS Workshop on Lung Volume Measurements. Official Statement of The European Respiratory Society. *Eur Respir J.* 1995;8(3):492-506.

26. Quanjer PH, Tammeling GJ, Cotes JE, Pedersen OF, Peslin R, Yernault JC. Lung volumes and forced ventilatory flows. *Eur Respir J.* 1993;6 Suppl 16:5-40.

27. Macintyre N, Crapo RO, Viegi G, et al. Standardisation of the single-breath determination of carbon monoxide uptake in the lung. *Eur Respir J.* 2005;26(4):720-735.

28. Modi P, Cascella M. Diffusing Capacity Of The Lungs For Carbon Monoxide. *StatPearls*. Treasure Island (FL): StatPearls Publishing; 2022.

29. Lange P, Halpin DM, O'Donnell DE, MacNee W. Diagnosis, assessment, and phenotyping of COPD: beyond FEV_1. *Int J Chron Obstruct Pulmon Dis.* 2016;11 Spec Iss(Spec Iss):3-12.

30. Jones PW, Quirk FH, Baveystock CM, Littlejohns P. A self-complete measure of health status for chronic airflow limitation. The St. George's Respiratory Questionnaire. *Am Rev Respir Dis.* 1992;145(6):1321-1327.

31. Jones PW. St. George's Respiratory Questionnaire: MCID. *Copd.* 2005;2(1):75-79.

32. Enright PL. The six-minute walk test. *Respir Care.* 2003;48(8):783-785.

33. ATS statement: guidelines for the six-minute walk test. *Am J Respir Crit Care Med.* 2002;166(1):111-117.

34. Bell M, Fotheringham I, Punekar YS, Riley JH, Cockle S, Singh SJ. Systematic Review of the Association Between Laboratory- and Field-Based Exercise Tests and Lung Function in Patients with Chronic Obstructive Pulmonary Disease. *Chronic Obstr Pulm Dis.* 2015;2(4):321-342.

35. Karanth MS, Awad NT. Six Minute Walk Test: A Tool for Predicting Mortality in Chronic Pulmonary Diseases. *J Clin Diagn Res.* 2017;11(4):Oc34-oc38.

36. Nakano Y, Muro S, Sakai H, et al. Computed tomographic measurements of airway dimensions and emphysema in smokers. Correlation with lung function. *Am J Respir Crit Care Med.* 2000;162(3 Pt 1):1102-1108.

37. Gevenois PA, De Vuyst P, de Maertelaer V, et al. Comparison of computed density and microscopic morphometry in pulmonary emphysema. *Am J Respir Crit Care Med.* 1996;154(1):187-192.

38. Newell JD, Jr., Sieren J, Hoffman EA. Development of quantitative computed tomography lung protocols. *J Thorac Imaging.* 2013;28(5):266-271.

39. Kirby M, Pike D, McCormack DG, Lam S, Coxson HO, Parraga G. Longitudinal Computed Tomography and Magnetic Resonance Imaging of COPD: Thoracic Imaging Network of Canada (TINCan) Study Objectives. *Chronic Obstr Pulm Dis.* 2014;1(2):200-211.

40. Government of Canada. Canadian Nuclear Safety Commission Radiation Doses. 2020.

41. (NCRP) NCoRPaM. *Ionizing Radiation Exposure of the Population of the United States.* Vol Report No. 1602009.

42. Kirby M, Tanabe N, Vasilescu DM, et al. Computed Tomography Total Airway Count Is Associated with the Number of Micro-Computed Tomography Terminal Bronchioles. *Am J Respir Crit Care Med.* 2020;201(5):613-615.

43. Lynch DA, Al-Qaisi MA. Quantitative computed tomography in chronic obstructive pulmonary disease. *J Thorac Imaging.* 2013;28(5):284-290.

44. Murphy K, Pluim JP, van Rikxoort EM, et al. Toward automatic regional analysis of pulmonary function using inspiration and expiration thoracic CT. *Med Phys.* 2012;39(3):1650-1662.

45. Pompe E, Strand M, van Rikxoort EM, et al. Five-year Progression of Emphysema and Air Trapping at CT in Smokers with and Those without Chronic Obstructive Pulmonary Disease: Results from the COPDGene Study. *Radiology.* 2020;295(1):218-226.

46. Matsuoka S, Kurihara Y, Yagihashi K, Hoshino M, Watanabe N, Nakajima Y. Quantitative assessment of air trapping in chronic obstructive pulmonary disease using inspiratory and expiratory volumetric MDCT. *AJR Am J Roentgenol.* 2008;190(3):762-769.

47. Gevenois PA, de Maertelaer V, De Vuyst P, Zanen J, Yernault JC. Comparison of computed density and macroscopic morphometry in pulmonary emphysema. *Am J Respir Crit Care Med.* 1995;152(2):653-657.

48. Cerveri I, Dore R, Corsico A, et al. Assessment of emphysema in COPD: a functional and radiologic study. *Chest.* 2004;125(5):1714-1718.

49. Martinez CH, Chen YH, Westgate PM, et al. Relationship between quantitative CT metrics and health status and BODE in chronic obstructive pulmonary disease. *Thorax.* 2012;67(5):399-406.

50. Han MK, Kazerooni EA, Lynch DA, et al. Chronic obstructive pulmonary disease exacerbations in the COPDGene study: associated radiologic phenotypes. *Radiology.* 2011;261(1):274-282.

51. Roos JE, McAdams HP, Kaushik SS, Driehuys B. Hyperpolarized Gas MR Imaging: Technique and Applications. *Magn Reson Imaging Clin N Am.* 2015;23(2):217-229.

52. Kirby M, Heydarian M, Svenningsen S, et al. Hyperpolarized 3He magnetic resonance functional imaging semiautomated segmentation. *Acad Radiol.* 2012;19(2):141-152.

53. Donnelly LF, MacFall JR, McAdams HP, et al. Cystic fibrosis: combined hyperpolarized 3He-enhanced and conventional proton MR imaging in the lung--preliminary observations. *Radiology.* 1999;212(3):885-889.

54. Woodhouse N, Wild JM, Paley MN, et al. Combined helium-3/proton magnetic resonance imaging measurement of ventilated lung volumes in smokers compared to never-smokers. *J Magn Reson Imaging.* 2005;21(4):365-369.

55. McMahon CJ, Dodd JD, Hill C, et al. Hyperpolarized 3helium magnetic resonance ventilation imaging of the lung in cystic fibrosis: comparison with high resolution CT and spirometry. *Eur Radiol.* 2006;16(11):2483-2490.

56. Lui JK, LaPrad AS, Parameswaran H, Sun Y, Albert MS, Lutchen KR. Semiautomatic segmentation of ventilated airspaces in healthy and asthmatic subjects using hyperpolarized 3He MRI. *Comput Math Methods Med.* 2013;2013:624683.

57. Zha W, Niles DJ, Kruger SJ, et al. Semiautomated Ventilation Defect Quantification in Exercise-induced Bronchoconstriction Using Hyperpolarized Helium-3 Magnetic Resonance Imaging: A Repeatability Study. *Acad Radiol.* 2016;23(9):1104-1114.

58. Hughes PJC, Horn FC, Collier GJ, Biancardi A, Marshall H, Wild JM. Spatial fuzzy c-means thresholding for semiautomated calculation of percentage lung ventilated volume from hyperpolarized gas and (1) H MRI. *J Magn Reson Imaging.* 2018;47(3):640-646.

59. Kirby M, Wheatley A, McCormack D, Parraga G. *Development and application of methods to quantify spatial and temporal hyperpolarized 3He MRI ventilation dynamics: preliminary results in chronic obstructive pulmonary disease.* Vol 7626: SPIE; 2010.

60. Tustison NJ, Avants BB, Flors L, et al. Ventilation-based segmentation of the lungs using hyperpolarized (3)He MRI. *J Magn Reson Imaging.* 2011;34(4):831-841.

61. He M, Kaushik SS, Robertson SH, et al. Extending semiautomatic ventilation defect analysis for hyperpolarized (129)Xe ventilation MRI. *Acad Radiol.* 2014;21(12):1530-1541.

62. Tustison NJ, Avants BB, Lin Z, et al. Convolutional Neural Networks with Template-Based Data Augmentation for Functional Lung Image Quantification. *Acad Radiol.* 2019;26(3):412-423.

63. Kirby M, Svenningsen S, Owrangi A, et al. Hyperpolarized 3He and 129Xe MR imaging in healthy volunteers and patients with chronic obstructive pulmonary disease. *Radiology.* 2012;265(2):600-610.

64. Kirby M, Pike D, Sin DD, Coxson HO, McCormack DG, Parraga G. COPD: Do Imaging Measurements of Emphysema and Airway Disease Explain Symptoms and Exercise Capacity? *Radiology.* 2015;277(3):872-880.

65. Kirby M, Eddy RL, Pike D, et al. MRI ventilation abnormalities predict quality-of-life and lung function changes in mild-to-moderate COPD: longitudinal TINCan study. *Thorax.* 2017;72(5):475-477.

66. Eddy RL, Svenningsen S, McCormack DG, Parraga G. What is the Minimal Clinically Important Difference for ³He MRI Ventilation Defects? *European Respiratory Journal.* 2018:1800324.

67. Fain SB, Panth SR, Evans MD, et al. Early emphysematous changes in asymptomatic smokers: detection with 3He MR imaging. *Radiology.* 2006;239(3):875-883.

68. Kaushik SS, Cleveland ZI, Cofer GP, et al. Diffusion-weighted hyperpolarized 129Xe MRI in healthy volunteers and subjects with chronic obstructive pulmonary disease. *Magn Reson Med.* 2011;65(4):1154-1165.

69. Hartroft WS. The Microscopic Diagnosis of Pulmonary Emphysema. *Am J Pathol.* 1945;21(5):889-903.

70. Quirk JD, Lutey BA, Gierada DS, et al. In vivo detection of acinar microstructural changes in early emphysema with (3)He lung morphometry. *Radiology.* 2011;260(3):866-874.

71. Ley S, Zaporozhan J, Morbach A, et al. Functional evaluation of emphysema using diffusion-weighted 3Helium-magnetic resonance imaging, high-resolution computed tomography, and lung function tests. *Invest Radiol.* 2004;39(7):427-434.

72. van Beek EJ, Dahmen AM, Stavngaard T, et al. Hyperpolarised 3He MRI versus HRCT in COPD and normal volunteers: PHIL trial. *Eur Respir J.* 2009;34(6):1311-1321.

73. Nakano Y, Wong JC, de Jong PA, et al. The prediction of small airway dimensions using computed tomography. *Am J Respir Crit Care Med.* 2005;171(2):142-146.

74. Grydeland TB, Dirksen A, Coxson HO, et al. Quantitative computed tomography measures of emphysema and airway wall thickness are related to respiratory symptoms. *Am J Respir Crit Care Med.* 2010;181(4):353-359.

75. Kirby M, Tanabe N, Tan WC, et al. Total Airway Count on Computed Tomography and the Risk of Chronic Obstructive Pulmonary Disease Progression. Findings from a Population-based Study. *Am J Respir Crit Care Med.* 2018;197(1):56-65.

76. Kirby M, Smith BM, Tanabe N, et al. Computed tomography total airway count predicts progression to COPD in at-risk smokers. *ERJ Open Res.* 2021;7(4).

77. Smith BM, Hoffman EA, Rabinowitz D, et al. Comparison of spatially matched airways reveals thinner airway walls in COPD. The Multi-Ethnic Study of Atherosclerosis (MESA) COPD Study and the Subpopulations and Intermediate Outcomes in COPD Study (SPIROMICS). *Thorax*. 2014;69(11):987-996.

CHAPTER 2

2 REDUCED TOTAL AIRWAY COUNT AND AIRWAY WALL TAPERING AFTER THREE-YEARS IN EX-SMOKERS

To better understand disease progression and the longitudinal pathophysiological changes in COPD, we evaluated and compared CT airway measurements in ex-smokers with and without COPD over three-years.

2.1 Introduction

Chronic obstructive pulmonary disease (COPD) is characterized by chronic airflow obstruction,[1] parenchymal lung destruction, and airway abnormalities.[2] For decades, spirometry has provided the key clinical measurements for COPD diagnosis and management.[1] However, spirometry measurements made at the mouth cannot estimate regional airway or parenchymal abnormalities, especially potential abnormalities in the distal, small airways, where disease onset and progression are hypothesized to initiate.[3]

Thoracic CT serves as the clinical mainstay for COPD imaging and imaging phenotypes, including terminal airspace enlargement or emphysema[4] and airways disease[5] and has been utilized in numerous cohort studies including MESA,[6] ECLIPSE,[7] COPDGene,[8] SPIROMICS,[9] and CanCOLD.[10] Segmentation of the CT airway tree from the trachea down to approximately the 6-10th generation airways provides a way to measure total airway count (TAC) and airway wall and lumen dimensions. CT airway abnormalities may be quantified using a number of different algorithms[11-14] and these abnormalities have been shown to be related to respiratory symptoms[15] and to reflect small airway dimensions measured using histo-pathological approaches.[16]

Previous work demonstrated that CT TAC may be quantified in patients with COPD.[17] TAC was observed to be diminished across COPD grade severity[17] and was associated with the number of terminal bronchioles measured with micro-CT,[18] while predictive of incident COPD in at-risk ever-smokers.[19] Airway wall dimension differences were also observed across COPD grade severity[20] and these were spatially related to missing airways.[17]

While all of this important information about airway wall thickness and airway count provide a way to understand differences in patients with different COPD severities, it is still unclear how TAC and airway wall thickness change over time in individual patients or within disease severity subgroups. Longitudinal changes that may occur in the airways of ex-smokers, especially in those with normal pulmonary function, may provide insights into COPD initiation and progression. Longitudinal Thoracic Imaging Network of Canada (TINCan) ^{3}He MRI[21-23] and small vessel density[24] findings were previously described. Based on cross-sectional findings in a number of cohort studies,[17-20] here we hypothesized that, even in the absence of FEV_1 worsening, CT airway measurements would significantly worsen in ex-smokers with and without spirometry or other evidence of COPD. Hence, our primary objective was to evaluate longitudinal CT airway measurements in a relatively large group of ex-smokers in the TINCan cohort study[21] after three-years.

2.2 Materials and Methods

2.2.1 Study Participants and Design

All participants provided written informed consent to an ethics-board, (Institutional Ethics Board #00000984) Health Canada approved and registered (ClinicalTrials.gov: NCT02279329) protocol. Inclusion criteria included a history of combustible tobacco cigarette smoking ≥10 pack-years and age of 50-85 years at baseline, while exclusion criteria consisted of claustrophobia and any contraindications for MRI or CT and current smokers. Ex-smokers were included who ceased smoking at least one-year prior to the study visit with no maximum cut-off for pack-years. COPD was defined as post-bronchodilator spirometry according to the Global Initiative for Chronic Obstructive Lung Disease (GOLD) criteria.[1]

This study was prospectively planned and participants for this analysis were enrolled from January 2010 to July 2016. All participants underwent two, two-hour visits for pulmonary function tests, quality-of-life questionnaires, six-minute walk test, MRI, and CT.[21] Follow-up was prospectively planned for 24±6 months after the baseline visit. All evaluations were performed 20 minutes after administering Novo-Salbutamol HFA using a metered dose inhaler (four doses of 100 ug, Teva Novopharm Ltd., Toronto, Ontario, Canada) through a

spacer (AeroChamber Plus spacer, Trudell Medical International, London, Ontario, Canada).

2.2.2 Pulmonary Function Tests and Questionnaires

Spirometry, plethysmography, and measurement of the diffusing capacity of the lung for carbon monoxide were performed according to American Thoracic Society/European Respiratory Society guidelines[25-27] using a body plethysmograph (MedGraphics Elite Series, MGC Diagnostic Corporation, St. Paul, Minnesota, USA) with an attached gas analyzer. St. George's Respiratory Questionnaire was administered,[28] and a six-minute walk test was also performed,[29] under supervision of trained personnel.

2.2.3 Image Acquisition

Anatomic ^{1}H and hyperpolarized ^{3}He ventilation MRI were acquired on a 3T Discovery MR750 system (GE Healthcare, Milwaukee, Wisconsin, USA), as previously described.[30] Anatomic ^{1}H MRI was acquired using a whole-body radiofrequency coil and a fast-spoiled gradient-recalled echo (FGRE) sequence during inspiration breath-hold from functional residual capacity, as previously described.[30] ^{3}He MRI was acquired using a single-channel rigid elliptical transmit-receive chest coil (RAPID Biomedical, Wuerzburg, Germany) and an FGRE sequence during inspiration breath-hold, as previously described.[30]

Within 30 minutes of MRI, CT was acquired on a 64-slice Lightspeed VCT scanner (GE Healthcare, Milwaukee, Wisconsin, USA) under breath-hold after inhalation of 1L of N_2 from functional residual capacity, as previously described.[21] CT images were acquired with the following parameters: beam collimation of 64×0.625mm, 120kVp, effective mAs of 100, 500ms tube rotation time, 1.25 pitch, and image reconstruction with a standard convolution kernel to 1.25mm. Total effective dose was estimated as 1.8mSv using the ImPACT CT patient dosimetry calculator (based on Health Protection Agency [UK] NRBP-SR250).

2.2.4 Image Analysis

^{3}He MRI ventilation defect percent (VDP) was measured using semi-automated segmentation pipeline generated in MATLAB R2019a (MathWorks, Natick, Massachusetts, USA), as previously described.[31]

Thoracic CT images were analyzed using VIDAvision software (VIDA Diagnostics Inc., Coralville, Iowa, USA) to segment the lungs and airway tree by a single trained observer (PVW, 2 years of experience). As previously described,[17] all airway segments in the segmented airway tree were summed to quantify TAC. Anatomically equivalent segmental, subsegmental, and sub-subsegmental airways for all airway paths (third to fifth generation) [20] were used to generate airway lumen area (LA), wall area (WA), wall area percent (WA%), and wall thickness percent (WT%). Emphysema was quantified using the relative area of the segmented lung with attenuation values less than -950 Hounsfield units (RA_{950}).

2.2.5 Statistics

Statistics were generated using SPSS (ver. 28; IBM Statistics, Armonk, New York, USA). Data were tested for normality using Shapiro-Wilk tests and non-parametric tests were performed when data were not normally distributed. Independent samples t-tests and analysis of variance were used to determine significance of between-group differences. Paired samples t-tests were used to determine significance between time points. Univariate relationships were evaluated using Pearson (r) correlations for normally distributed variables and Spearman (ρ) correlations for non-normally distributed variables. Variables with significant correlation *P* values at baseline were used to generate multivariable models, where significant variables included in the model were chosen using the backward approach, to predict TAC at three-year follow-up. The removal criterion for the backwards method included variables with a probability of $F \geq 0.10$. Multicollinearity among variables in the multivariable regression models was evaluated using the variance inflation factor and deemed acceptable when less than 10.[32] Results were considered statistically significant when the probability of making a type I error was less than 5% ($P<.05$).

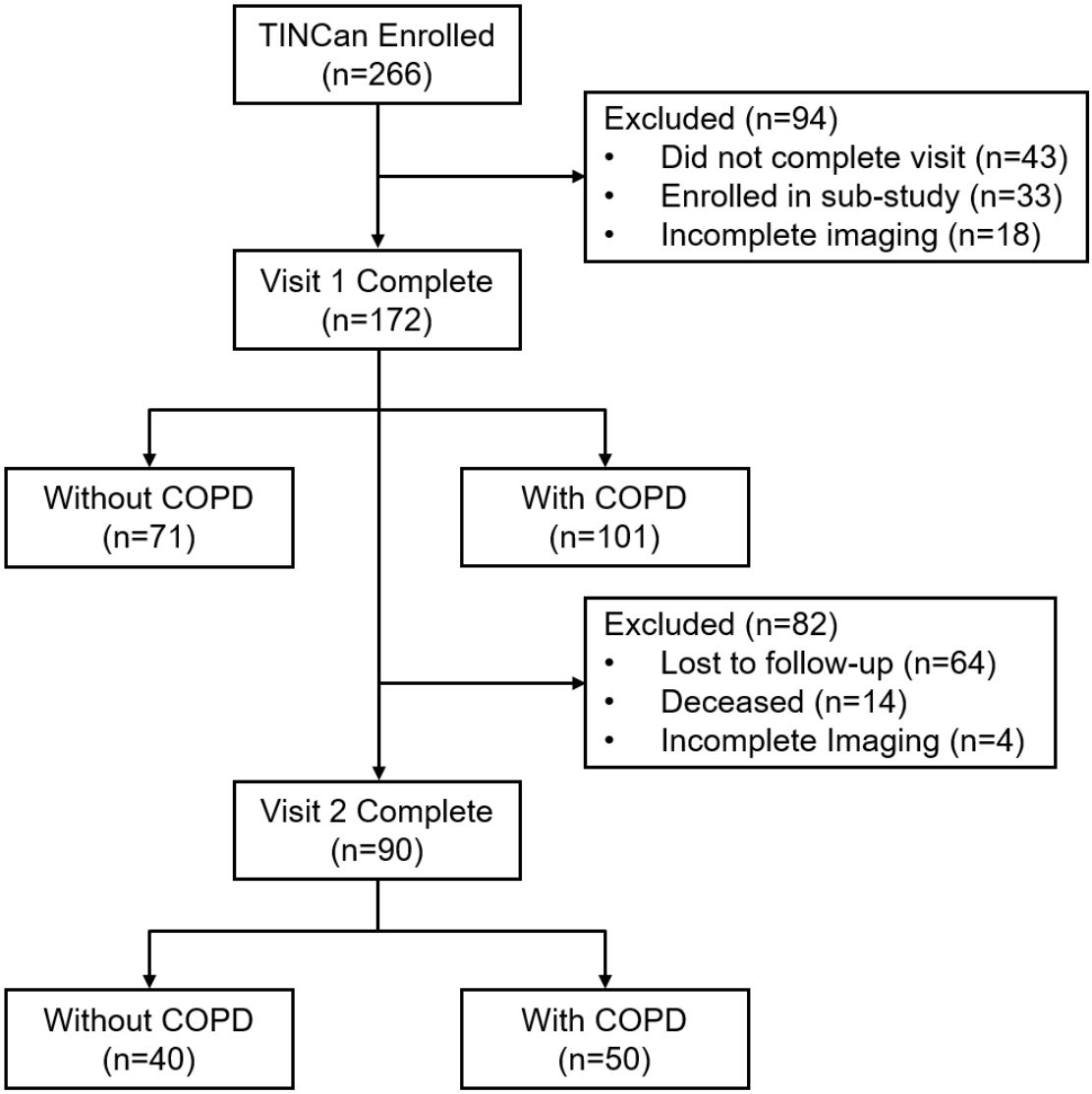

Figure 2.1: CONSORT diagram for TINCan cohort study.
Of the 266 enrolled, 172 ex-smokers with and without chronic obstructive pulmonary disease (COPD) completed the baseline visit (Visit 1), while 90 ex-smokers completed the follow-up visit (Visit 2) and were included in the analysis.

2.3 Results

A CONSORT diagram for the Thoracic Imaging Network of Canada (TINCan) study provided in **Figure 2.1** shows that 266 participants were enrolled and 172 participants completed all imaging examinations at baseline. Of those participants who did not complete Visit 1, some withdrew after consent (n=43), some were enrolled in a sub-study of oscillatory positive expiratory pressure (n=33),[33] and some could not complete imaging

measurements (n=18) due to claustrophobia, poor coil fit, or radiation dose concerns. After 31±7 months, 90 participants returned for a complete follow-up Visit 2. Of those who were excluded from Visit 2 analysis, 64 were lost to follow-up, 14 were deceased, and four had CT data which were not evaluable because of motion artifacts.

Table 2.1: Participant demographics for ex-smokers with and without COPD, at baseline and three-year follow-up

	All Ex-smokers n=90			**Without COPD n=40**			**With COPD n=50**		
Parameter	**Baseline**	**Follow-up**	***P***	**Baseline**	**Follow-up**	***P***	**Baseline**	**Follow-up**	***P***
Age [y]	70 (9)	72 (9)	ND	69 (10)	72 (10)	ND	70 (9)	73 (9)	ND
Female [n (%)]	30 (33)	30 (33)	ND	17 (43)	17 (43)	ND	13 (26)	13 (26)	ND
BMI [kg/m^2]	28 (4)	28 (5)	.6	30 (4)	30 (4)	.6	27 (4)	26 (4)	.1
SaO_2 [%]	95 (3)	95 (3)	.9	95 (5)	96 (2)	.9	95 (2)	94 (3)	**.01**
Pack-years	38 (23)	38 (23)	ND	31 (17)	31 (17)	ND	43 (26)	43 (26)	ND
FU time [m]	-	31 (7)	ND	-	31 (5)	ND	-	31 (8)	ND

Values are reported as mean (SD) unless otherwise indicated. *P* values represent significance values for paired samples and paired proportions t-tests. Bolded values are statistically significant.
BMI=body mass index; COPD=Chronic Obstructive Pulmonary Disease; GOLD=Global Initiative for Chronic Obstructive Lung Disease; ND=not done; SaO_2=oxygen saturation.

Table 2.2: Participant demographics for ex-smokers with COPD according to GOLD grade, at baseline and three-year follow-up

	GOLD I n=16			**GOLD II n=24**			**GOLD III/IV n=10**		
Parameter	**Baseline**	**Follow-up**	***P***	**Baseline**	**Follow-up**	***P***	**Baseline**	**Follow-up**	***P***
Age [y]	74 (8)	76 (8)	ND	68 (8)	70 (8)	ND	69 (10)	71 (10)	ND
Female [n (%)]	1 (6)	1 (6)	ND	9 (38)	9 (38)	ND	3 (30)	3 (30)	ND
BMI [kg/m^2]	28 (4)	28 (4)	.3	26 (4)	26 (3)	.7	27 (6)	26 (5)	.1
SaO_2 [%]	96 (1)	95 (3)	.3	95 (3)	94 (3)	**.003**	95 (2)	95 (3)	.9
Pack-years	37 (26)	37 (26)	ND	44 (20)	44 (20)	ND	51 (37)	51 (37)	ND
FU time [m]	-	29 (4)	ND	-	33 (9)	ND	-	29 (8)	ND

Values are reported as mean (SD) unless otherwise indicated. *P* values represent uncorrected significance values for paired samples t-tests. Bolded values are statistically significant.
BMI=body mass index; COPD=Chronic Obstructive Pulmonary Disease; GOLD=Global Initiative for Chronic Obstructive Lung Disease; ND=not done; SaO_2=oxygen saturation.

2.3.1 Demographics

Table 2.1 shows demographics for all 90 participants including ex-smokers with spirometry evidence of COPD (n=50; mean age, 70±9years [SD]; 37 male, 13 female) and ex-smokers without COPD (n=40; mean age, 69±10years [SD]; 23 male, 17 female). As shown in Table 1, after three-years, there was a significant but small difference in resting oxygen saturation (95%/94%; *P*=.01) in ex-smokers with COPD, but not in ex-smokers without COPD. **Table 2.2** provides participant demographics by GOLD grade severity and shows that there was a significant but small difference in resting oxygen saturation (95%/94%; *P*=.003) only in ex-smokers with GOLD II grade COPD.

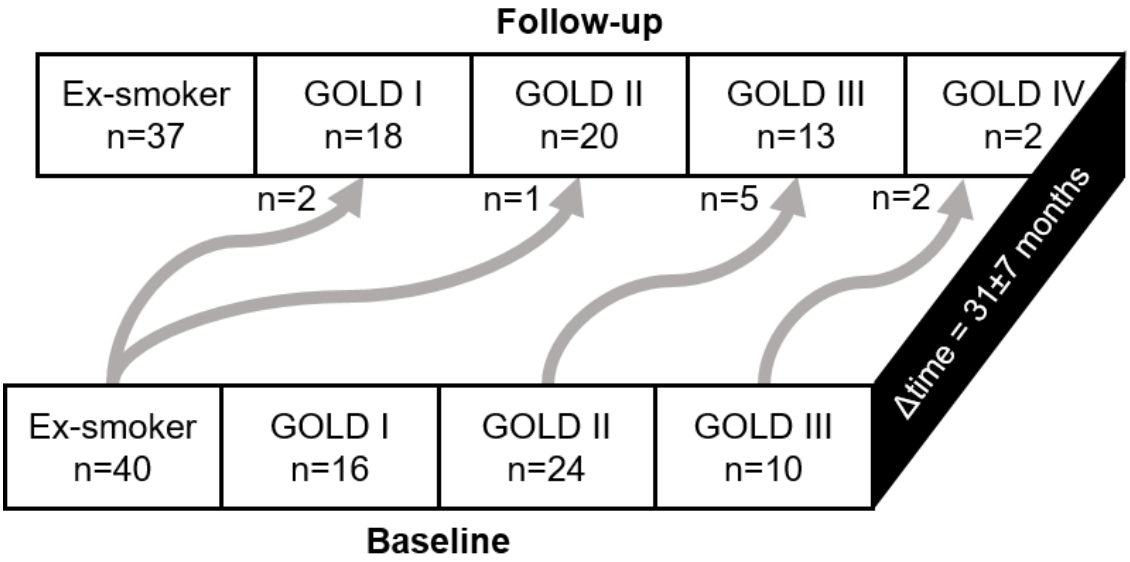

Figure 2.2: Diagram of COPD severity progression for all ex-smokers.
Arrows showing progression in severity at follow-up for ex-smokers without COPD (n=40) and ex-smokers with COPD (n=50) within GOLD grade subgroups. Of the 40 ex-smoker participants at baseline, two transitioned to GOLD I at follow-up and one transitioned to GOLD II. Of the 24 GOLD II participants, five transitioned to GOLD III. Of the 10 GOLD III participants, two transitioned to GOLD IV.

Figure 2.2 shows COPD grade severity progression at follow-up for all participants. Of the 40 ex-smoker participants at baseline, two transitioned to GOLD I at follow-up and one transitioned to GOLD II. The ex-smoker who transitioned to GOLD II had an abnormal FEV_1 (60%) and a preserved ratio of FEV_1 to forced vital capacity (FVC) (77%) at baseline, which was abnormal (63%) at follow-up. Of the 24 GOLD II participants, five transitioned to GOLD III. Of the 10 GOLD III participants, two transitioned to GOLD IV.

Table 2.3 shows baseline measurements for ex-smokers who did not return for follow-up (n=82) compared to those who did (n=90). Those who did not return for follow-up reported significantly worse FEV_1 (68%/84%; *P*<.001), FVC (84%/95%; *P*=.003), FEV_1/FVC (59%/65%; *P*=.02), RV (152%/127%; *P*<.001), RV/TLC (51%/44%; *P*<.001), DL_{CO} (59%/67%; *P*=.02), 6MWD (366m/400m; *P*=.02), and SGRQ (40/29; *P*=.003) as compared to those that returned.

Table 2.3: Participant demographics, pulmonary function, exercise capacity, and quality-of-life measurements at baseline for ex-smokers with and without COPD who did not return for follow-up and for those who did return for follow-up

	Baseline Ex-smokers without Follow-up			**Baseline Ex-smokers with Follow-up**			
Parameter	**All n=82**	**ES n=31**	**COPD n=51**	**All n=90**	**ES n=40**	**COPD n=50**	***P***
Age [y]	69 (10)	69 (10)	70 (9)	70 (9)	70 (10)	70 (9)	.6
Females [n (%)]	36 (44)	14 (45)	22 (43)	29 (32)	16 (40)	13 (26)	ND
BMI [kg/m^2]	27 (5)	28 (4)	26 (5)	28 (4)	30 (4)	27 (4)	**.03**
SaO_2 [%]	95 (3)	96 (2)	95 (3)	95 (3)	95 (5)	95 (2)	.9
Pack-years	39 (26)	25 (14)	48 (28)	38 (23)	31 (17)	43 (26)	.8
FEV_1 [$\%_{pred}$]	68 (30)	95 (19)	52 (23)	84 (27)	103 (18)	69 (23)	**<.001**
FVC [$\%_{pred}$]	84 (19)	89 (17)	82 (20)	95 (17)	95 (17)	95 (18)	**.003**
FEV_1/FVC [%]	59 (20)	79 (7)	46 (13)	65 (17)	81 (6)	53 (11)	**.02**
RV* [$\%_{pred}$]	152 (52)	112 (28)	177 (48)	127 (41)	106 (20)	143 (44)	**<.001**
TLC* [$\%_{pred}$]	114 (20)	100 (15)	122 (18)	109 (16)	102 (12)	114 (17)	.09
RV/TLC* [%]	51 (12)	43 (9)	55 (10)	44 (10)	40 (8)	47 (11)	**<.001**
DL_{CO}* [$\%_{pred}$]	59 (25)	77 (25)	48 (17)	67 (21)	78 (17)	59 (21)	**.02**
6MWD* [m]	366 (99)	404 (89)	340 (99)	400 (83)	401 (99)	400 (72)	**.02**
SGRQ*	40 (23)	26 (24)	48 (19)	30 (20)	22 (20)	36 (19)	**.003**

Values are reported as mean (SD) unless otherwise indicated. One-way ANOVA was used to test for differences between participants at baseline who did not attend the follow-up visit (n=82) and those that did attend the follow-up visit (n=90).
P values represent significantly values. Bolded values are statistically significant.
$\%_{pred}$=percent of predicted value; 6MWD=six-minute walk distance; BMI=body mass index; COPD=Chronic Obstructive Pulmonary Disease; DL_{CO}=diffusing capacity of the lung for carbon monoxide; FEV_1=forced expiratory volume in one second; FVC=forced vital capacity; GOLD=Global Initiative for Chronic Obstructive Lung Disease; ND=not done; RV=residual volume; SaO_2=oxygen saturation; SGRQ=St. George's Respiratory Questionnaire; TLC=total lung capacity.

RV*, TLC*, RV/TLC*: Baseline ex-smokers with follow-up n=89
DL_{CO}*: Baseline ex-smokers without follow-up n=81, Baseline ex-smokers with follow-up n=88
6MWD*: Baseline ex-smokers without follow-up n=72, Baseline ex-smokers with follow-up n=89
SGRQ*: Baseline ex-smokers without follow-up n=79, Baseline ex-smokers with follow-up n=84

2.3.2 Longitudinal Pulmonary Function and Imaging Measurements

Representative CT emphysema (threshold of -950 Hounsfield units is shown in yellow) and segmented airway tree images at baseline and three-year follow-up for ex-smokers with and without COPD are shown in **Figure 2.3**. In the ex-smoker without COPD, at both time points, there was no CT evidence of emphysema, nor diminished TAC. In the ex-smoker with GOLD I grade COPD, at both time points, there was small evidence of emphysema and TAC was visually diminished compared to the ex-smoker without COPD. In the ex-smoker with GOLD II grade COPD, emphysema was visually obvious in the lower lobes at baseline, whilst at follow-up, emphysema extent was visibly augmented in the left lower lobe and TAC was visually diminished. In the ex-smoker with GOLD III grade COPD, there was widespread emphysema in both upper and lower lobes which was visually obviously increased at follow-up. At baseline and follow-up, TAC was substantially diminished compared to the ex-smoker without COPD.

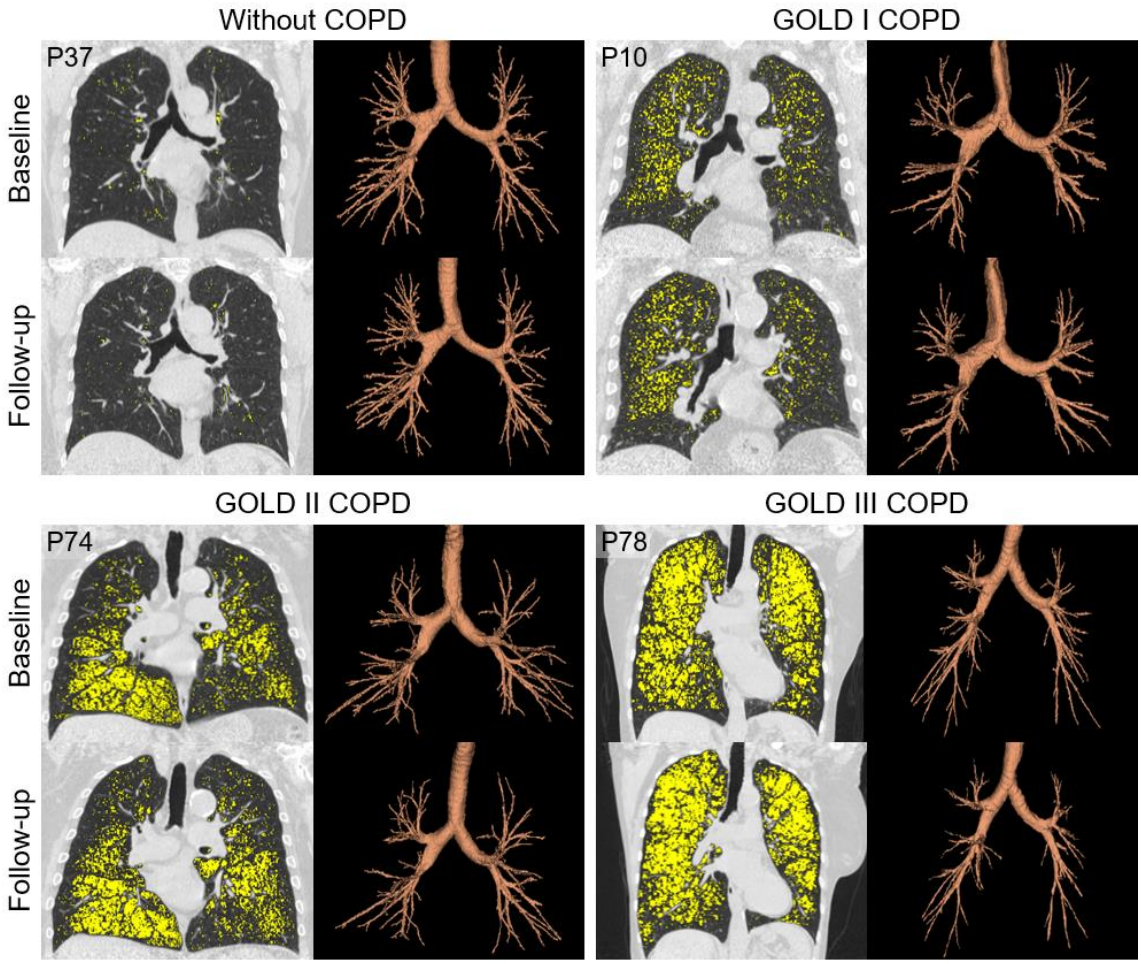

Figure 2.3: Baseline and three-year follow-up CT imaging for representative ex-smokers with and without COPD.

P37 is a 70 year old female ex-smoker without COPD, with follow-up time = 31 months (baseline/follow-up: FEV_1 $\%_{pred}$ = 93%/93%; RA_{950} = 1%/1%; TAC = 306/297). P10 is a 75 year old male ex-smokers with GOLD I COPD, with follow-up time = 33 months (baseline/follow-up: FEV_1 $\%_{pred}$ = 92%/84%; RA_{950} = 7%/8%; TAC = 265/231). P74 is an 83 year old male ex-smoker with GOLD II COPD, with follow-up time = 28 months (baseline/follow-up: FEV_1 $\%_{pred}$ = 57%/52%; RA_{950} = 20%/23%; TAC = 258/191). P78 is a 67 year old female ex-smoker with GOLD III COPD, with follow-up time = 26 months (baseline/follow-up: FEV_1 $\%_{pred}$ = 37%/33%; RA_{950} = 33%/37%; TAC = 206/174).
Left: Coronal CT reconstruction with RA_{950} shown in yellow. Right: Three-dimensional reconstruction of the segmented airway tree.

Table 2.4: Pulmonary function, questionnaire, and imaging measurements for ex-smokers with and without COPD, at baseline and three-year follow-up

	All Ex-smokers n=90			Without COPD n=40			With COPD n=50		
Parameter	**Baseline**	**Follow-up**	***P***	**Baseline**	**Follow-up**	***P***	**Baseline**	**Follow-up**	***P***
Lung Function									
FEV_1 [$\%_{pred}$]	84 (27)	84 (30)	.9	103 (18)	104 (20)	.5	69 (23)	68 (26)	.4
FVC [$\%_{pred}$]	95 (17)	94 (20)	.4	95 (17)	97 (18)	.2	95 (18)	92 (21)	**.04**
FEV_1/FVC [%]	65 (17)	64 (16)	.1	81 (6)	79 (7)	**.01**	53 (11)	53 (12)	.6
RV* [$\%_{pred}$]	126 (40)	126 (40)	.9	106 (20)	103 (20)	.4	143 (44)	145 (42)	.6
TLC* [$\%_{pred}$]	109 (16)	104 (20)	**.01**	102 (12)	97 (2)	**<.001**	114 (17)	112 (16)	.4
RV/TLC* [%]	44 (10)	45 (12)	.4	40 (8)	42 (8)	.07	47 (11)	48 (12)	.4
DL_{CO}* [$\%_{pred}$]	68 (21)	72 (25)	**.003**	79 (15)	87 (17)	**<.001**	60 (20)	60 (24)	.4
Exercise and QoL									
6MWD* [m]	412 (76)	396 (85)	**.006**	420 (81)	407 (77)	**.049**	405 (72)	387 (91)	**.049**
SGRQ*	29 (20)	29 (21)	.9	22 (20)	21 (19)	.7	65 (19)	63 (21)	.7
CT									
RA_{950} [%]	5.8 (7.6)	7.8 (8.9)	**<.001**	1.5 (1.4)	2.0 (1.5)	**.02**	9.2 (8.8)	12.5 (9.7)	**<.001**
TAC [n]	270 (81)	252 (78)	**<.001**	306 (87)	297 (82)	.2	241 (63)	217 (52)	**<.001**
WA [mm^2]	66.6 (1.9)	66.3 (1.7)	**.02**	65.8 (2.0)	65.5 (1.7)	.2	67.2 (1.5)	66.9 (1.5)	**.04**
LA [mm^2]	14.6 (3.6)	15.6 (3.6)	**<.001**	16.1 (4.0)	17.0 (3.7)	**.009**	13.3 (2.7)	14.5 (3.1)	**<.001**
WA% [%]	82.2 (4.0)	81.0 (3.9)	**<.001**	80.4 (4.4)	79.5 (3.9)	**.01**	83.5 (3.0)	82.3 (3.4)	**<.001**
WT% [%]	17.8 (0.8)	17.6 (0.8)	**<.001**	17.6 (0.8)	17.5 (0.7)	.07	18.0 (0.7)	17.7 (0.8)	**<.001**
MRI									
VDP* [%]	12.2 (9.4)	15.8 (11.9)	**<.001**	6.4 (3.6)	8.6 (4.8)	**.002**	16.8 (10.1)	21.3 (12.9)	**<.001**

Values are reported as mean (SD) unless otherwise indicated. *P* values represent significance values for paired samples t-tests. Bolded values are statistically significant. $\%_{pred}$=percent of predicted value; 6MWD=six-minute walk distance; COPD=Chronic Obstructive Pulmonary Disease; DL_{CO}=diffusing capacity of the lung for carbon monoxide; FEV_1=forced expiratory volume in 1-second; FVC=forced vital capacity; LA=lumen area; QoL=quality of life; RA_{950}=relative area of the lung with attenuation less than -950 Hounsfield units; RV=residual volume; SGRQ=St. George's Respiratory Questionnaire; TAC=total airway count; TLC=total lung capacity; VDP=ventilation defect percent; WA=wall area; WA%=wall area percent; WT%=wall thickness percent.

Table 2.4 shows pulmonary function, exercise capacity, quality-of-life, and imaging measurements at baseline and three-year follow-up; similar information is provided by GOLD grade severity in **Table 2.5**. In ex-smokers without COPD, after three-years, there were significant differences in FEV_1/FVC (81%/79%; *P*=.01), total lung capacity (102%/97%; *P*<.001), diffusing capacity of the lung (79%/87%; *P*<.001), and six-minute walk distance (420m/407m; *P*=.049). In addition, the relative area of the lung with attenuation <-950 Hounsfield units (RA_{950}) (1.5%/2.0%; *P*=.02), airway LA ($16.1mm^2$/$17.0mm^2$; *P*=.009), WA% (80.4%/79.5%; *P*=.01), and VDP (6.4%/8.6%; *P*=.002) were different, three-years after the baseline visit. In ex-smokers with COPD, there was a significant difference in FVC (95%/92%; *P*=.04), six-minute walk distance

(405m/387m; *P*=.049), RA_{950} (9.2%/12.5%; *P*<.001), TAC (241/217; *P*<.001), airway WA ($67.2mm^2$/$66.9mm^2$; *P*=.04), LA ($13.3mm^2$/$14.5mm^2$; *P*<.001), WA% (83.5%/82.3%; *P*<.001), WT% (18.0%/17.7%; *P*<.001), and VDP (16.8%/21.3%; *P*<.001).

Table 2.5: Pulmonary function, questionnaire, and imaging measurements for all ex-smokers and for those with COPD according to GOLD grade, at baseline and three-year follow-up

	GOLD I n=16			GOLD II n=24			GOLD III/IV n=10		
Parameter	**Baseline**	**Follow-up**	***P***	**Baseline**	**Follow-up**	***P***	**Baseline**	**Follow-up**	***P***
Lung Function									
FEV_1 [$\%_{pred}$]	97 (12)	99 (12)	.4	62 (8)	59 (13)	.08	39 (8)	37 (8)	.2
FVC [$\%_{pred}$]	110 (13)	112 (14)	.6	94 (13)	89 (12)	**.02**	74 (10)	66 (16)	.1
FEV_1/FVC [%]	64 (4)	64 (5)	.8	50 (9)	50 (10)	.6	40 (7)	42 (9)	.3
RV* [$\%_{pred}$]	117 (30)	117 (20)	1.0	138 (28)	144 (32)	.2	204 (46)	178 (76)	.3
TLC* [$\%_{pred}$]	110 (13)	109 (11)	.6	112 (16)	112 (18)	1.0	125 (22)	108 (42)	.2
RV/TLC* [%]	39 (8)	41 (6)	.4	47 (9)	49 (8)	.1	60 (8)	52 (26)	.3
DL_{CO}* [$\%_{pred}$]	74 (20)	78 (22)	.2	58 (20)	56 (20)	.6	43 (10)	42 (20)	.9
Exercise and QoL									
6MWD* [m]	422 (49)	409 (62)	.4	411 (73)	400 (98)	.4	362 (89)	322 (92)	**.03**
SGRQ*	23 (18)	21 (19)	.4	35 (15)	37 (16)	.6	53 (15)	54 (18)	.6
CT									
RA_{950} [%]	3.7 (3.2)	6.3 (4.0)	**.001**	11.3 (9.7)	14.4 (10.5)	**<.001**	13.3 (8.7)	17.7 (9.8)	**.004**
TAC [n]	250 (65)	230 (55)	**.002**	236 (71)	211 (56)	**.001**	237 (42)	209 (38)	**.005**
WA [mm^2]	66.7 (1.4)	66.2 (1.4)	**.049**	67.6 (1.7)	67.3 (1.4)	.2	67.1 (1.3)	67.0 (1.6)	.9
LA [mm^2]	13.8 (2.9)	15.2 (3.2)	**.01**	12.9 (2.3)	14.1 (2.6)	**.005**	13.4 (3.2)	14.3 (4.2)	.2
WA% [%]	82.9 (3.2)	81.4 (3.5)	**.01**	84.0 (2.7)	82.8 (2.9)	**.009**	83.5 (3.5)	82.5 (4.5)	.3
WT% [%]	17.8 (0.7)	17.5 (0.8)	.07	18.2 (0.7)	17.7 (0.8)	**.003**	17.9 (0.7)	17.9 (0.9)	.7
MRI									
VDP* [%]	7.5 (3.3)	10.9 (4.2)	**.002**	17.5 (7.7)	22.0 (10.4)	**.001**	29.4 (8.1)	35.8 (13.5)	**.049**

Values are reported as mean (SD) unless otherwise indicated. *P* values represent significance values for paired samples t-tests. Bolded values are statistically significant.
$\%_{pred}$=percent of predicted value; 6MWD=six-minute walk distance; COPD=Chronic Obstructive Pulmonary Disease; DL_{CO}=diffusing capacity of the lung for carbon monoxide; FEV_1=forced expiratory volume in one second; FVC=forced vital capacity; GOLD=Global Initiative for Chronic Obstructive Lung Disease; LA=lumen area; QoL=quality of life; RA_{950}=relative area of the lung with attenuation less than -950 Hounsfield units; RV=residual volume; SGRQ=St. George's Respiratory Questionnaire; TAC=total airway count; TLC=total lung capacity; VDP=ventilation defect percent; WA=wall area; WA%=wall area percent; WT%=wall thickness percent.

RV*, TLC*, RV/TLC*: GOLD III/IV n=9
DL_{CO}*: GOLD II n=22, GOLD III/IV n=9
6MWD*: GOLD I n=15, GOLD II n=22, GOLD III/IV n=9
SGRQ*: GOLD I n=15
VDP*: GOLD I n=14, GOLD III/IV n=9

CT airway measurements summarized in scatter plots in **Figure 2.4** show that TAC significantly decreased in ex-smokers with COPD, but not in ex-smokers without COPD and that WA% decreased in both ex-smoker subgroups. **Figure 2.5** provides similar information by COPD grade severity and shows that TAC decreased in all COPD grade severity subgroups, while WA% decreased only in GOLD I and GOLD II subgroups. **Figure 2.6** provides a schematic summarizing the changes observed after three-years for TAC, airway WA, LA, WA%, WT%, and VDP in both ex-smoker subgroups.

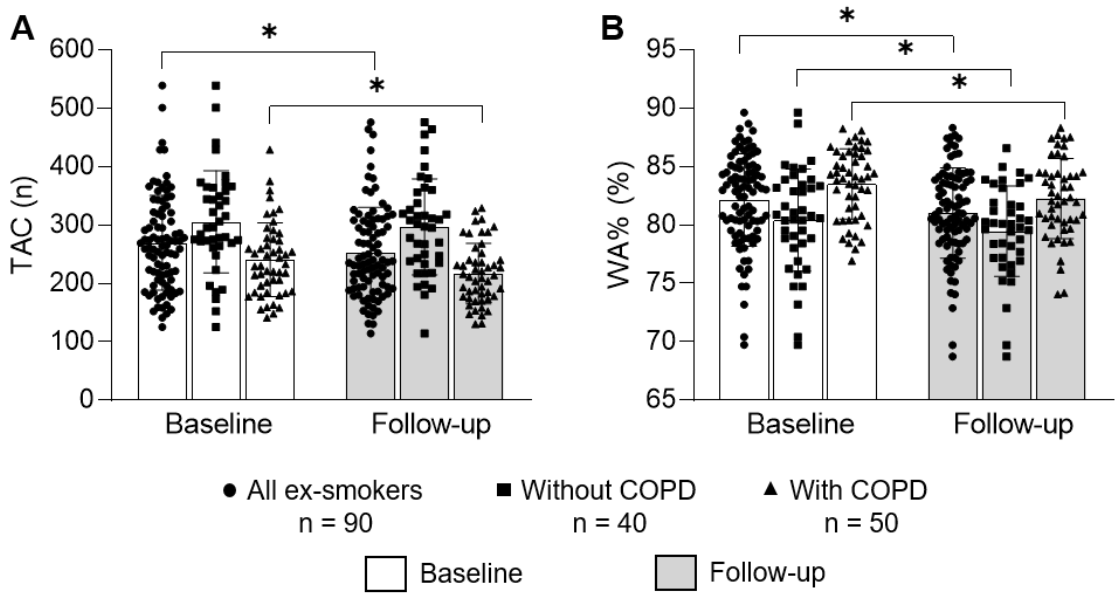

Figure 2.4: Scatter plots with bars showing CT airway measurements for ex-smokers with and without COPD, at baseline and three-year follow-up.
(A) Scatter plot with bars shows total TAC at baseline and follow-up for all ex-smokers (270/252; *P*<.001) and ex-smokers with COPD (241/217; *P*<.001). **(B)** Scatter plot with bars shows airway WA% at baseline and follow-up for all ex-smokers (82.2%/81.0%; *P*<.001), ex-smokers without COPD (80.4%/79.5%; *P*=.01), and ex-smokers with COPD (83.5%/82.3%; *P*<.001). Asterisks indicate significant differences (*P*<.05), circles indicate measurements of individual ex-smokers, squares indicate measurements of individual ex-smokers without COPD, triangles indicate individual ex-smokers with COPD, white bars indicate baseline measurements, and grey bars indicate follow-up measurements.

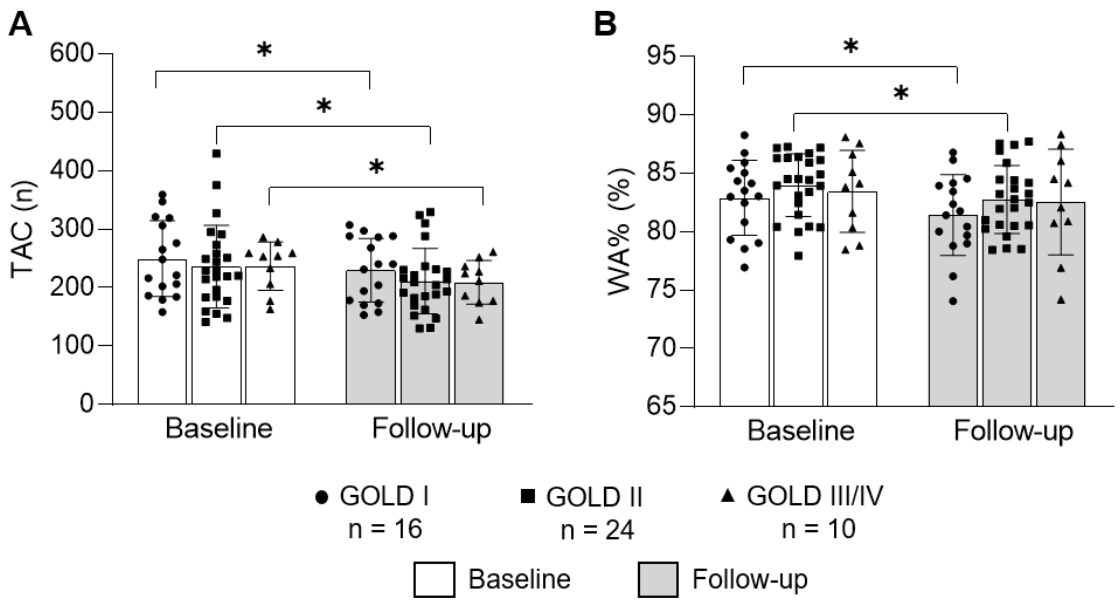

Figure 2.5: Scatter plots with bars showing CT airway measurements for ex-smokers with COPD within GOLD grade subgroups, at baseline and three-year follow-up.
(A) Scatter plot with bars shows TAC at baseline and follow-up for ex-smokers with GOLD I COPD (250/230; *P*=.002), ex-smokers with GOLD II COPD (236/211; *P*=.001), and ex-smokers with GOLD III/IV COPD (237/209; *P*=.005). **(B)** Scatter plot with bars shows airway WA% at baseline and follow-up for ex-smokers with GOLD I COPD (82.9%/81.4%; *P*=.01) and ex-smokers with GOLD II COPD (84.0%/82.8%; *P*=.009). Asterisks indicate significant differences (*P*<.05), circles indicate measurements of individual ex-smokers, squares indicate measurements of individual ex-smokers without COPD, triangles indicate individual ex-smokers with COPD, white bars indicate baseline measurements, and grey bars indicate follow-up measurements.

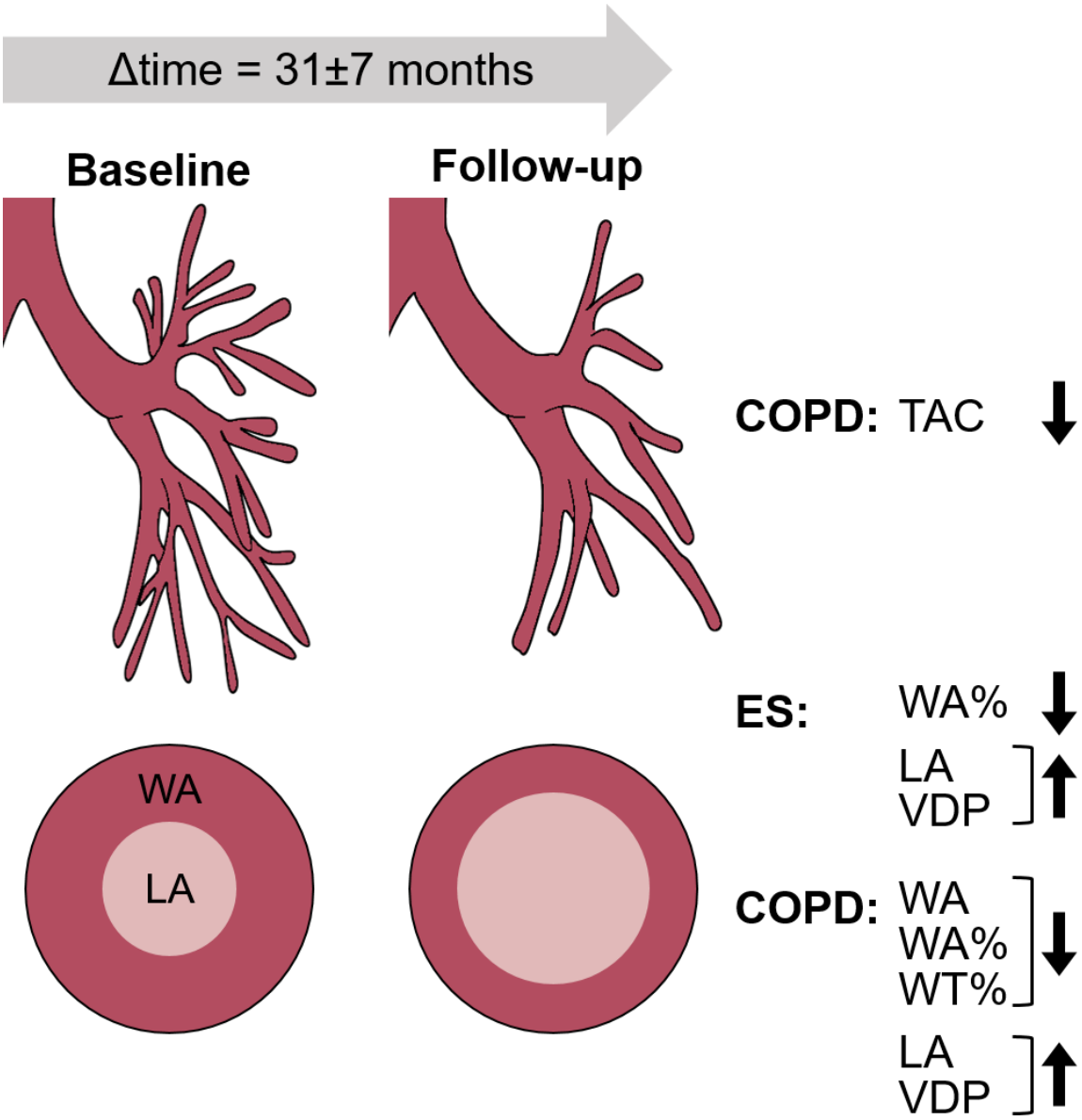

Figure 2.6: Schematic of CT airway measurement changes over three-years in ex-smokers with and without COPD.
Schematic showing decreased total airway count (TAC) in ex-smokers with chronic obstructive pulmonary disease (COPD). Schematic also shows decreased airway wall area percent (WA%) and increased lumen area (LA) and ventilation defect percent (VDP) in ex-smokers without COPD (ES), as well as decreased airway wall area (WA), WA% and wall thickness percent (WT%), and increased LA and VDP in ex-smokers with COPD.

2.3.3 Relationships

Figure 2.7 shows baseline and follow-up correlations for TAC with FEV_1 (baseline: ρ=.38, *P*<.001; follow-up: ρ=.48, *P*<.001) and VDP (baseline: ρ=-.30, *P*=.005; follow-up: ρ=-.33, *P*=.002).

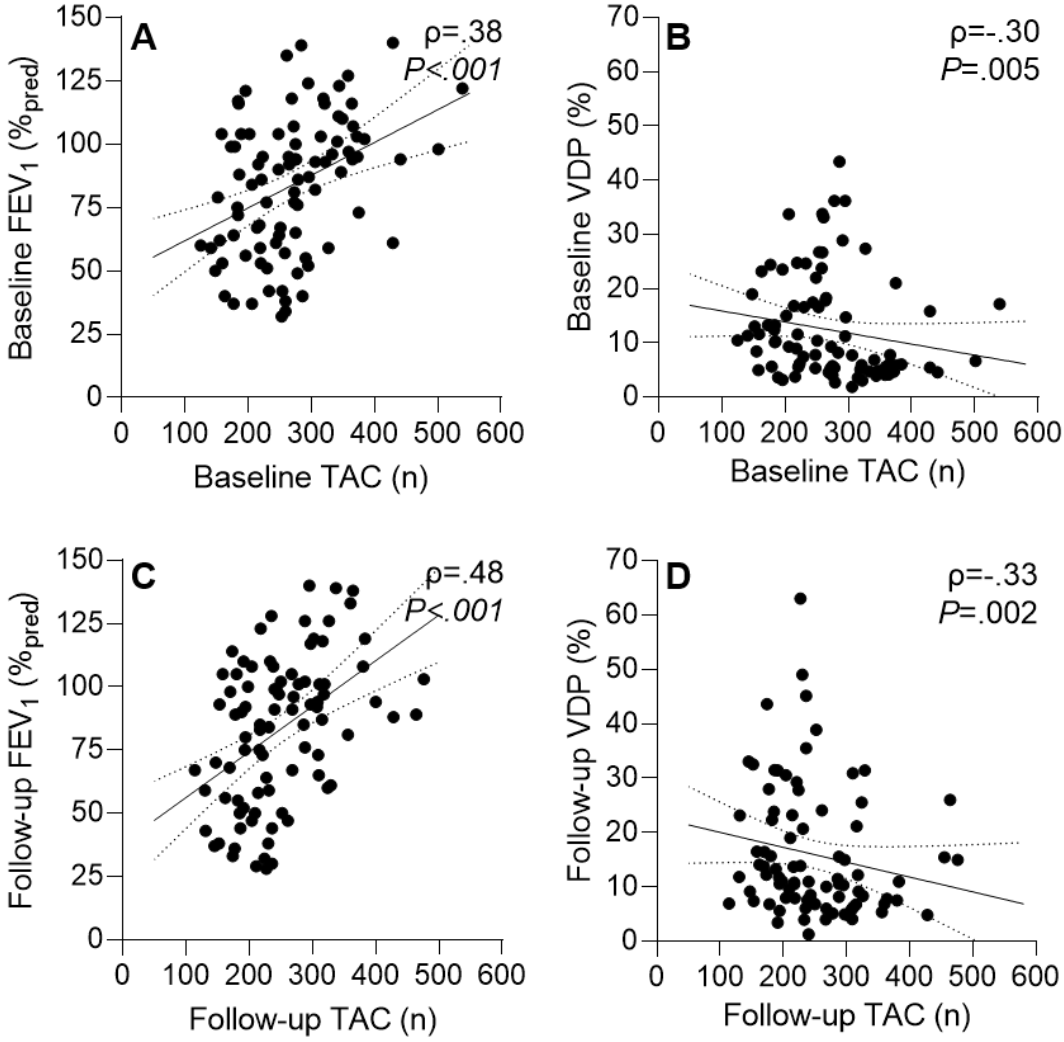

Figure 2.7: Scatter plots showing relationships at baseline and follow-up in all ex-smokers.
(A) Scatter plot shows TAC was correlated with FEV_1 (ρ=.38, *P*<.001) at baseline. **(B)** Scatter plot shows TAC was correlated with VDP (ρ=-.30, *P*=.005) at baseline. **(C)** Scatter plot shows TAC was correlated with FEV_1 (ρ=.48, *P*<.001) at follow-up. **(D)** Scatter plot shows TAC was correlated with VDP (ρ=-.33, *P*=.002) at follow-up.

We also generated multivariable models to predict TAC at three-year follow-up and these are shown in **Table 2.6**, while **Table 2.7** shows correlation values for potential predictor variables. The variance inflation factors were acceptable for all variables included in the multivariate models. In the best model (R^2=.632; *P*<.001), WA% (β=-0.625; *P*<.001) and FEV_1/FVC (β=0.300; *P*<.001) at baseline were significant predictors of TAC at follow-up, while residual volume to total lung capacity ratio (β=-0.018; *P*=.8), relative area of the lung with attenuation <-950 Hounsfield units (β=-0.039; *P*=.7), VDP (β=-0.029; *P*=.8), diffusing capacity of the lung (β=0.010; *P*=.9), FEV_1 (β=0.045; *P*=.7), and WT% (β=0.195; *P*=.2) were excluded.

Table 2.6: Multivariable Linear Regression Models for TAC at Follow-up

	Unstandardized		Standardized	
Parameter	**B**	**SE**	**β**	***P***
TAC at follow-up				
Best Model*				
Constant	1155.783	125.374	-	
WA%	-12.106	1.400	-0.625	**<.001**
FEV_1/FVC	1.376	.331	0.300	**<.001**
Excluded				
RV/TLC			-0.018	.820
RA_{950}			-0.039	.674
VDP			-0.029	.773
DL_{CO} $\%_{pred}$			0.010	.898
FEV_1 $\%_{pred}$			0.045	.674
WT%			0.195	.180

P values show coefficient significance. Bolded values are statistically significant. All prediction variables represent measurements at baseline.
%pred=percent of predicted value; DL_{CO}=diffusing capacity of the lung for carbon monoxide; FEV_1=forced expiratory volume in 1-second; FVC=forced vital capacity; RA_{950}=relative area of the lung with attenuation less than -950 Hounsfield units; RV=residual volume; TAC=total airway count; TLC=total lung capacity; VDP=ventilation defect percent; WA%=wall area percent; WT%=wall thickness percent.
*R^2 = .632; *P* < .001

Table 2.7: Correlations for Potential Predictor Variables in Linear Regression Models

	TAC at baseline	
Predictor variables at baseline	**ρ**	***P***
FEV_1 $\%_{pred}$	.38	**<.001**
FVC $\%_{pred}$	-.01	.9
FEV_1/FVC	.47	**<.001**
RV $\%_{pred}$	-.35	**<.001**
TLC $\%_{pred}$	-.21	**.045**
RV/TLC	-.25	**.02**
DL_{CO} $\%_{pred}$	.21	**.046**
6MWD	.09	.4
SGRQ	-.18	.1
VDP	-.30	**.005**
RA_{950}	-.23	**.03**
WA	-.76	**<.001**
LA	.74	**<.001**
WA%	-.75	**<.001**
WT%	-.62	**<.001**

P value represents significance values for Pearson and spearman correlations. Bolded values are statistically significant.

%pred=percent of predicted value; 6MWD=six-minute walk distance; DL_{CO}=diffusing capacity of the lung for carbon monoxide; FEV_1=forced expiratory volume in 1-second; FVC=forced vital capacity; LA=lumen area; ρ=Spearman correlation coefficient; r=Pearson correlation coefficient; RA_{950}=relative area of the lung with attenuation less than -950 Hounsfield units; RV=residual volume; SGRQ=St. George's Respiratory Questionnaire; TAC=total airway count; TLC=total lung capacity; VDP=ventilation defect percent; WA=wall area; WA%=wall area percent; WT%=wall thickness percent.

2.4 Discussion

Previous quantitative CT studies revealed that total airway count (TAC)[17] and airway wall dimensions [20] were significantly different across chronic obstructive pulmonary disease (COPD) Global Initiative for Chronic Obstructive Lung Disease (GOLD) grades. To more deeply investigate these previous cross-sectional findings, we quantitatively evaluated CT airway measurements at baseline and after three-years in ex-smokers who took part in the Thoracic Imaging Network of Canada (TINCan) cohort. We observed: 1) significantly decreased TAC (241/217; $P<.001$) in ex-smokers with spirometry evidence of COPD, but not in those without, 2) a small but significant change in airway wall area (WA) ($67.2mm^2/66.9mm^2$; $P=.04$), lumen area (LA) ($13.3mm^2/14.5mm^2$; $P<.001$), wall area percent (WA%) (83.5%/82.3%; $P<.001$) and wall thickness percent (WT%) (18.0%/17.7%; $P<.001$) in ex-smokers with COPD, as well as in LA ($16.1mm^2/17.0mm^2$; $P=.009$) and WA% (80.4%/79.5%; $P=.01$) in ex-smokers without COPD, 3) a significant relationship between CT TAC and MRI ventilation defect percent (VDP) (baseline: $\rho=-.30$, $P=.005$; follow-up: $\rho=-.33$, $P=.002$), and, 4) in a significant multivariable model ($R^2=.632$; $P<.001$), baseline WA% ($\beta=-0.625$; $P<.001$) and forced expiratory volume in 1-second (FEV_1) to forced vital capacity (FVC) ratio ($\beta=0.300$; $P<.001$) predicted TAC at follow-up.

Approximately three-years after a baseline visit, TAC was decreased in ex-smokers with COPD and by GOLD grade, but not in ex-smokers without COPD. We cannot ascertain the cause of this decrease in CT-visible airways, including potential technical issues, airway narrowing, occlusion, obstruction, and/or obliteration. We do know however, that CT TAC was previously shown to be associated with the number of micro-CT terminal bronchioles,[18] lending support to the notion that differences in TAC may reflect small airway loss or obliteration. We also know from previous work that TAC explained COPD progression,[19] so perhaps by measuring TAC over time, we can better understand or predict which patients will worsen more quickly over time.

Regardless of COPD diagnosis, WA% was diminished in ex-smokers, suggestive of airway wall thinning over time, and this result was consistent with previous cross-sectional findings.[20] It is important to note that in previous work, airways with thinner walls were

spatially related to missing airways[17] in COPD, whereas in asthma, missing airways were spatially related to airways with thicker walls.[34] It is possible that CT airway wall thinning stems from progressive airway destruction over time in COPD whereas in asthma, airway inflammation and remodelling play a larger role.

We also observed LA enlarged over time in all ex-smokers, suggestive of luminal dilation. Previous studies have shown that the airway lumen is more narrow in ever-smokers with COPD compared to healthy controls.[17] Here we also observed a narrower lumen in ex-smokers with COPD compared to those without. We were surprised to observe airway luminal area increasing over time. Perhaps this was simply the result of survivor airway remodelling, reflecting that the mechanisms leading to luminal narrowing may change upon smoking cessation, as previously hypothesized.[35]

We observed a significant relationship between TAC and FEV_1, consistent with previous findings.[17] TAC was also negatively correlated with VDP, suggesting that for ex-smokers with reduced CT-visible airways, ventilation heterogeneity is greater (worse) which intuitively makes sense. Moreover, both MRI VDP and CT wall and lumen measurements changed over three-years in the absence of changes in FEV_1, which suggests that these airway changes occur before they are reflected by spirometry measurements, which are dominated by the large airways. Importantly, previous work demonstrated that TAC was associated with the longitudinal six-year decline in FEV_1.[17] In agreement with this finding, the best performing multivariable model we generated also identified baseline WA% and FEV_1/FVC as significant predictors of TAC at follow-up. In fact, these two variables together explained more than 60% of the variability of TAC in these participants over time. We were surprised that baseline MRI VDP, while correlating with TAC, did not significantly contribute to the most predictive model. Instead, thicker airway walls and/or narrower lumen at baseline were associated with lower TAC at follow-up. Moreover, ex-smokers with diminished FEV_1/FVC at baseline (who were more obstructed), also had diminished TAC at follow-up. Thus, for those participants in whom TAC significantly worsened after three-years, baseline CT airway and spirometry measurements were supportive baseline predictors.

We acknowledge a number of study limitations including the relatively small sample size especially compared to other COPD cohort studies.[6-10] In addition, the study participants were recruited as a convenience and not a random population-based sample which may have biased the results to people who were in better (or worse) health at baseline. This study was also dominated by patients with an absence of, or milder COPD. Participants who attended a baseline visit but who did not return for follow-up reported worse values for pulmonary function, exercise capacity and quality-of-life compared to those who did return. Taken together, this result suggests that this study provides a relatively conservative estimate of potential longitudinal differences.

In summary, over a relatively short time period of 31±7 months, we observed reduced CT total airway count in ex-smokers with chronic obstructive pulmonary disease (COPD), as well as airway wall thinning in all ex-smokers. These longitudinal findings in ex-smokers in whom there was no forced expiratory volume in 1-second worsening provide insights into mechanisms of COPD progression, whilst supporting previous cross-sectional evaluations.[17,20]

2.5 References

1. Global Initiative for Chronic Obstructive Lung Disease (GOLD). Global Strategy for the Diagnosis, Mangement and Prevention of Chronic Obstructive Pulmonary Disease: 2022 Report. 2021.

2. McDonough JE, Yuan R, Suzuki M, et al. Small-airway obstruction and emphysema in chronic obstructive pulmonary disease. *N Engl J Med.* 2011;365(17):1567-1575.

3. Hogg JC, Macklem PT, Thurlbeck WM. Site and nature of airway obstruction in chronic obstructive lung disease. *N Engl J Med.* 1968;278(25):1355-1360.

4. Gevenois PA, De Vuyst P, de Maertelaer V, et al. Comparison of computed density and microscopic morphometry in pulmonary emphysema. *Am J Respir Crit Care Med.* 1996;154(1):187-192.

5. Nakano Y, Muro S, Sakai H, et al. Computed tomographic measurements of airway dimensions and emphysema in smokers. Correlation with lung function. *Am J Respir Crit Care Med.* 2000;162(3 Pt 1):1102-1108.

6. Bild DE, Bluemke DA, Burke GL, et al. Multi-Ethnic Study of Atherosclerosis: objectives and design. *Am J Epidemiol.* 2002;156(9):871-881.

7. Vestbo J, Anderson W, Coxson HO, et al. Evaluation of COPD Longitudinally to Identify Predictive Surrogate End-points (ECLIPSE). *Eur Respir J.* 2008;31(4):869-873.

8. Regan EA, Hokanson JE, Murphy JR, et al. Genetic epidemiology of COPD (COPDGene) study design. *COPD.* 2010;7(1):32-43.

9. Couper D, LaVange LM, Han M, et al. Design of the Subpopulations and Intermediate Outcomes in COPD Study (SPIROMICS). *Thorax.* 2014;69(5):491-494.

10. Bourbeau J, Tan WC, Benedetti A, et al. Canadian Cohort Obstructive Lung Disease (CanCOLD): Fulfilling the need for longitudinal observational studies in COPD. *COPD.* 2014;11(2):125-132.

11. McNitt-Gray MF, Goldin JG, Johnson TD, Tashkin DP, Aberle DR. Development and testing of image-processing methods for the quantitative assessment of airway hyperresponsiveness from high-resolution CT images. *J Comput Assist Tomogr.* 1997;21(6):939-947.

12. King GG, Müller NL, Whittall KP, Xiang QS, Paré PD. An analysis algorithm for measuring airway lumen and wall areas from high-resolution computed tomographic data. *Am J Respir Crit Care Med.* 2000;161(2 Pt 1):574-580.

13. Nakano Y, Whittall K, Kalloger S, et al. *Development and validation of human airway analysis algorithm using multidetector row CT.* Vol 4683: SPIE; 2002.

14. Orlandi I, Moroni C, Camiciottoli G, et al. Chronic obstructive pulmonary disease: thin-section CT measurement of airway wall thickness and lung attenuation. *Radiology.* 2005;234(2):604-610.

15. Grydeland TB, Dirksen A, Coxson HO, et al. Quantitative computed tomography measures of emphysema and airway wall thickness are related to respiratory symptoms. *Am J Respir Crit Care Med.* 2010;181(4):353-359.

16. Nakano Y, Wong JC, de Jong PA, et al. The prediction of small airway dimensions using computed tomography. *Am J Respir Crit Care Med.* 2005;171(2):142-146.

17. Kirby M, Tanabe N, Tan WC, et al. Total Airway Count on Computed Tomography and the Risk of Chronic Obstructive Pulmonary Disease Progression. Findings from a Population-based Study. *Am J Respir Crit Care Med.* 2018;197(1):56-65.

18. Kirby M, Tanabe N, Vasilescu DM, et al. Computed Tomography Total Airway Count Is Associated with the Number of Micro-Computed Tomography Terminal Bronchioles. *Am J Respir Crit Care Med.* 2020;201(5):613-615.

19. Kirby M, Smith BM, Tanabe N, et al. Computed tomography total airway count predicts progression to COPD in at-risk smokers. *ERJ Open Res.* 2021;7(4).

20. Smith BM, Hoffman EA, Rabinowitz D, et al. Comparison of spatially matched airways reveals thinner airway walls in COPD. The Multi-Ethnic Study of Atherosclerosis (MESA) COPD Study and the Subpopulations and Intermediate Outcomes in COPD Study (SPIROMICS). *Thorax.* 2014;69(11):987-996.

21. Kirby M, Pike D, McCormack DG, Lam S, Coxson HO, Parraga G. Longitudinal Computed Tomography and Magnetic Resonance Imaging of COPD: Thoracic Imaging Network of Canada (TINCan) Study Objectives. *Chronic Obstr Pulm Dis.* 2014;1(2):200-211.

22. Kirby M, Mathew L, Wheatley A, Santyr GE, McCormack DG, Parraga G. Chronic obstructive pulmonary disease: longitudinal hyperpolarized (3)He MR imaging. *Radiology.* 2010;256(1):280-289.

23. Kirby M, Eddy RL, Pike D, et al. MRI ventilation abnormalities predict quality-of-life and lung function changes in mild-to-moderate COPD: longitudinal TINCan study. *Thorax.* 2017;72(5):475-477.

24. Barker AL, Eddy RL, MacNeil JL, McCormack DG, Kirby M, Parraga G. CT Pulmonary Vessels and MRI Ventilation in Chronic Obstructive Pulmonary Disease: Relationship with worsening FEV_1 in the TINCan cohort study. *Acad Radiol.* 2021;28(4):495-506.

25. Miller MR, Hankinson J, Brusasco V, et al. Standardisation of spirometry. *Eur Respir J.* 2005;26(2):319-338.

26. Wanger J, Clausen JL, Coates A, et al. Standardisation of the measurement of lung volumes. *Eur Respir J.* 2005;26(3):511-522.

27. Macintyre N, Crapo RO, Viegi G, et al. Standardisation of the single-breath determination of carbon monoxide uptake in the lung. *Eur Respir J.* 2005;26(4):720-735.

28. Jones PW, Quirk FH, Baveystock CM, Littlejohns P. A self-complete measure of health status for chronic airflow limitation. The St. George's Respiratory Questionnaire. *Am Rev Respir Dis.* 1992;145(6):1321-1327.

29. Enright PL. The six-minute walk test. *Respir Care.* 2003;48(8):783-785.

30. Parraga G, Ouriadov A, Evans A, et al. Hyperpolarized 3He ventilation defects and apparent diffusion coefficients in chronic obstructive pulmonary disease: preliminary results at 3.0 Tesla. *Invest Radiol.* 2007;42(6):384-391.

31. Kirby M, Heydarian M, Svenningsen S, et al. Hyperpolarized 3He magnetic resonance functional imaging semiautomated segmentation. *Acad Radiol.* 2012;19(2):141-152.

32. O'brien RM. A Caution Regarding Rules of Thumb for Variance Inflation Factors. *Quality & Quantity.* 2007;41(5):673-690.

33. Svenningsen S, Paulin GA, Sheikh K, et al. Oscillatory Positive Expiratory Pressure in Chronic Obstructive Pulmonary Disease. *COPD.* 2016;13(1):66-74.

34. Eddy RL, Svenningsen S, Kirby M, et al. Is Computed Tomography Airway Count Related to Asthma Severity and Airway Structure and Function? *Am J Respir Crit Care Med.* 2020;201(8):923-933.

35. Willemse BW, Postma DS, Timens W, ten Hacken NH. The impact of smoking cessation on respiratory symptoms, lung function, airway hyperresponsiveness and inflammation. *Eur Respir J.* 2004;23(3):464-476.

CHAPTER 3

3 CONCLUSIONS AND FUTURE DIRECTIONS

In the previous chapter, the objectives and hypotheses of this thesis were addressed. In this final chapter, an overview and summary of the main findings are provided. Limitations specific to this study and future directions are also presented. Finally, the chapter concludes by discussing the significance and impact of this work on the field and the broader scientific community.

3.1 Overview and Research Questions

Thoracic CT serves as the gold-standard imaging approach in COPD, providing regional information regarding airway[1] and parenchymal[2] abnormalities, which cannot be estimated using spirometry measurements made at the mouth. Previous studies have shown diminished number of CT-visible airways[3] and thinner airway walls across COPD severities.[4] The purpose of this thesis was to evaluate these CT airway measurements longitudinally over three-years in a relatively large group of ex-smokers with and without COPD. I postulated that CT airway measurements would significantly worsen in ex-smokers, even in the absence of FEV_1 worsening. Through this work, I investigated longitudinal airway loss and airway wall thinning in ex-smokers, providing additional insights into COPD initiation and progression.

3.2 Summary and Conclusions

CT airway measurements at baseline and after three-years were evaluated and compared in a prospective convenience sample of 90 ex-smokers, including 50 with COPD and 40 without COPD. Over a relatively short time period of 31±7 months, FEV_1 was not significantly different in ex-smokers with (P=.4) and without (P=.5) COPD. Thus, in the absence of FEV_1 worsening, I demonstrated that there were significant differences in CT TAC (P<.001), airway WA (P=.04), LA (P<.001), WA% (P<.001), and WT% (P<.001) over three-years in ex-smokers with COPD; while LA (P=.009) and WA% (P=.01) were significantly different in ex-smokers without COPD. I also showed that CT TAC was correlated with FEV_1 (baseline: ρ=.38, P<.001; follow-up ρ=.48, P<.001) and MRI VDP

(baseline: ρ=-.30, *P*=.005; follow-up: ρ=-.33, *P*=.002) in all ex-smokers at both time points. Finally, in the best performing multivariable model (R^2=.632; *P*<.001), baseline CT WA% and FEV_1/FVC were identified as significant predictors of TAC at follow-up. Thus, I demonstrated that in participants with diminished TAC after three-years, CT airway wall and lumen dimensions and spirometry measurements were supportive baseline predictors.

Therefore, these longitudinal findings demonstrate that quantitative CT airway measurements, including TAC and airway wall and lumen dimensions, are important indicators of disease progression in COPD, while the clinical gold-standard of spirometry is not capable of capturing these airway structural changes over time.

3.3 Limitations

A limitation of this work is the relatively small sample size compared to other COPD cohort studies, such as COPDGene[5] and CanCOLD[6]. In addition, the study participants were recruited as a convenience and not a random population-based sample which may have biased the results to people who were in better health at baseline. As a result, this study was dominated by patients with an absence of, or milder COPD. However, participants who attended a baseline visit but who did not return for follow-up reported worse values for pulmonary function, exercise capacity, and quality-of-life compared to those who did return, suggesting that this study provides a relatively conservative estimate of potential longitudinal differences.

Another limitation of this work was the acquisition of CT images at FRC+1L instead of full inspiration, since this study was required to compromise between volume-matched MRI and CT acquisitions. On the basis of plethysmography data for the participants in this study, FRC+1L is equal to 80-90% of TLC, especially when the participant is lying supine in the scanner. Thus, such differences are within a few percent for RA_{950} values and are unlikely to be clinically relevant.[7] Nevertheless, CT emphysema estimates in participants in this study are similar to those in other published COPD studies.[4,8] We also did not acquire expiratory CT and therefore could not evaluate measurements of CT air trapping and their relationships with TAC and airway wall and lumen dimensions.

We think that decreased TAC over time has important implications for airways disease progression in COPD. However, these quantitative CT airway measurements are limited in their generalizability since they are dependent on the resolution of the CT system, as well as the observer performing airway segmentations. Thus, future work will need to evaluate the reproducibility of TAC in patients with COPD, as well as determine the minimal clinically important difference in TAC over time.

3.4 Future Directions

In the future, it would be important to evaluate CT mucus plugs in these participants at both time points and investigate potential relationships between mucus score and airway measurements. In COPD, chronic inflammation triggers mucus hypersecretion, which leads to luminal plugging and obstruction of the small airways, resulting in airway wall thickening.[9] Mucus symptoms such as chronic cough and sputum production are only present in a subset of patients with COPD and are associated with changes in the large airways.[10] However, these symptoms are often absent in patients who have pathologically proven mucus plugs. Dunican et al. developed a method for quantifying mucus plugs, which involves mucus scoring on thoracic CT images.[11] Previous work showed that the prevalence of mucus plugging is higher in smokers with COPD and increases across COPD grade severity.[12] This study also showed that mucus plugs are associated with decreased pulmonary function and worse quality of life. Another study showed that mucus plugs and emphysema are independently associated with lower FEV_1 and oxygen saturation.[13] Recently, a study showed that in segments containing mucus plugs as compared to those without, there was increased airway wall thickness and reduced airway counts on CT.[14]

Further, it would be interesting to follow-up these participants after a longer time period, to evaluate these longitudinal CT airway measurements and compare them with the findings presented in this thesis. In previous work evaluating five-year progression in smokers with and without COPD, CT emphysema and air trapping increased over this longer time period.[15] At a longer follow-up time of 10-years, pulmonary function, quality of life, and exercise capacity measurements appeared to progress slowly.[16] Furthermore, the rate of change in smokers without COPD closely mirrored that of those with COPD at all GOLD stages.[16] Therefore, in our cohort study, it would be interesting to see whether

TAC continues to decrease over a longer period of time in ex-smokers with COPD, if TAC eventually worsens in the ex-smokers without COPD, and if the rate of progression of CT airway measurements slows or worsens when comparing multiple time points.

Another important future direction for this work is to investigate the role of sex differences in the airways of the participants in this study and compare them with previous work completed in the COPDGene cohort,[17] as this is becoming an important consideration for the diagnosis and management of COPD.[18] In healthy never-smokers, men had thicker airways walls on CT compared to women, whereas airway lumen dimensions were lower in women than men, after accounting for height and lung size.[17] Similarly, in ever-smokers, women had narrower lumens as compared to men, and men had greater airway wall dimensions than women.[17] It would be interesting to determine whether our data will agree or expand upon these findings and if the longitudinal changes in CT airway measurements that we observed are different in women compared to men.

3.5 Significance and Impact

Structural airway remodeling and emphysematous destruction are key pathophysiological characteristics of COPD. For decades, spirometry has served as the clinical mainstay for diagnosis and management.[19] These global measurements made at the mouth cannot inform on regional lung abnormalities or on the heterogeneity of the disease. However, thoracic CT provides a way to visualize and quantify structural abnormalities in the lungs and has been exploited in many large COPD cohort studies. This thesis advances our understanding of COPD progression and significantly contributes to the literature as a novel study evaluating CT airway measurements over a three-year time period in ex-smokers.

My work provides evidence that ex-smokers, in the absence of FEV_1 worsening and regardless of COPD diagnosis, exhibit airway structural changes over time suggestive of airway wall thinning. Since previous work has shown an association between thinner airway walls and missing airways,[3] it is possible that CT airway wall thinning stems from progressive airway destruction over time in COPD. Furthermore, only ex-smokers with COPD exhibited airway count loss. To my knowledge, this is the first study to show CT TAC worsening over time in COPD. Since TAC was previously shown to be associated

with the number of micro-CT terminal bronchioles,[20] it stands to reason that patients with COPD experience small airway loss or obliteration over a relatively short time period of three-years. These longitudinal CT airway findings demonstrate that spirometry is insufficient in evaluating disease progression, adding to the value of quantitative CT in evaluating ex-smokers with and without COPD.

3.6 References

1. Nakano Y, Muro S, Sakai H, et al. Computed tomographic measurements of airway dimensions and emphysema in smokers. Correlation with lung function. *Am J Respir Crit Care Med.* 2000;162(3 Pt 1):1102-1108.

2. Gevenois PA, De Vuyst P, de Maertelaer V, et al. Comparison of computed density and microscopic morphometry in pulmonary emphysema. *Am J Respir Crit Care Med.* 1996;154(1):187-192.

3. Kirby M, Tanabe N, Tan WC, et al. Total Airway Count on Computed Tomography and the Risk of Chronic Obstructive Pulmonary Disease Progression. Findings from a Population-based Study. *Am J Respir Crit Care Med.* 2018;197(1):56-65.

4. Smith BM, Hoffman EA, Rabinowitz D, et al. Comparison of spatially matched airways reveals thinner airway walls in COPD. The Multi-Ethnic Study of Atherosclerosis (MESA) COPD Study and the Subpopulations and Intermediate Outcomes in COPD Study (SPIROMICS). *Thorax.* 2014;69(11):987-996.

5. Regan EA, Hokanson JE, Murphy JR, et al. Genetic epidemiology of COPD (COPDGene) study design. *COPD.* 2010;7(1):32-43.

6. Bourbeau J, Tan WC, Benedetti A, et al. Canadian Cohort Obstructive Lung Disease (CanCOLD): Fulfilling the need for longitudinal observational studies in COPD. *COPD.* 2014;11(2):125-132.

7. Madani A, Van Muylem A, Gevenois PA. Pulmonary emphysema: effect of lung volume on objective quantification at thin-section CT. *Radiology.* 2010;257(1):260-268.

8. Schroeder JD, McKenzie AS, Zach JA, et al. Relationships between airflow obstruction and quantitative CT measurements of emphysema, air trapping, and airways in subjects with and without chronic obstructive pulmonary disease. *AJR Am J Roentgenol.* 2013;201(3):W460-470.

9. Hogg JC. Pathophysiology of airflow limitation in chronic obstructive pulmonary disease. *Lancet.* 2004;364(9435):709-721.

10. Burgel P-R, Martin C. Mucus hypersecretion in COPD: should we only rely on symptoms? *European Respiratory Review.* 2010;19(116):94-96.

11. Dunican EM, Elicker BM, Gierada DS, et al. Mucus plugs in patients with asthma linked to eosinophilia and airflow obstruction. *J Clin Invest.* 2018;128(3):997-1009.

12. Okajima Y, Come CE, Nardelli P, et al. Luminal Plugging on Chest CT Scan: Association With Lung Function, Quality of Life, and COPD Clinical Phenotypes. *Chest.* 2020;158(1):121-130.

13. Dunican EM, Elicker BM, Henry T, et al. Mucus Plugs and Emphysema in the Pathophysiology of Airflow Obstruction and Hypoxemia in Smokers. *Am J Respir Crit Care Med.* 2021;203(8):957-968.

14. Tran C, Singh GV, Haider E, et al. Luminal mucus plugs are spatially associated with airway wall thickening in severe COPD and asthma: A single-centered, retrospective, observational study. *Respir Med.* 2022;202:106982.

15. Pompe E, Strand M, van Rikxoort EM, et al. Five-year Progression of Emphysema and Air Trapping at CT in Smokers with and Those without Chronic Obstructive Pulmonary Disease: Results from the COPDGene Study. *Radiology.* 2020;295(1):218-226.

16. Ragland MF, Strand M, Baraghoshi D, et al. 10-Year Follow-Up of Lung Function, Respiratory Symptoms, and Functional Capacity in the COPDGene Study. *Ann Am Thorac Soc.* 2022;19(3):381-388.

17. Bhatt SP, Bodduluri S, Nakhmani A, et al. Sex Differences in Airways at Chest CT: Results from the COPDGene Cohort. *Radiology.* 2022;305(3):699-708.

18. Raghavan D, Jain R. Increasing awareness of sex differences in airway diseases. *Respirology.* 2016;21(3):449-459.

19. Global Initiative for Chronic Obstructive Lung Disease (GOLD). Global Strategy for the Diagnosis, Mangement and Prevention of Chronic Obstructive Pulmonary Disease: 2022 Report. 2021.

20. Kirby M, Tanabe N, Vasilescu DM, et al. Computed Tomography Total Airway Count Is Associated with the Number of Micro-Computed Tomography Terminal Bronchioles. *Am J Respir Crit Care Med.* 2020;201(5):613-615.

Appendices

Appendix A: Health Science Research Ethics Board Approval Notices

Western Research

Date: 25 January 2022

To: Dr. Grace Parraga

Project ID: 6014

Study Title: Longitudinal Study of Helium-3 Magnetic Resonance Imaging of COPD

Application Type: Continuing Ethics Review (CER) Form

Review Type: Delegated

Date Approval Issued: 25/Jan/2022

REB Approval Expiry Date: 10/Feb/2023

Dear Dr. Grace Parraga,

The Western University Research Ethics Board has reviewed the application. This study, including all currently approved documents, has been re-approved until the expiry date noted above.

REB members involved in the research project do not participate in the review, discussion or decision.

Western University REB operates in compliance with, and is constituted in accordance with, the requirements of the Tri-Council Policy Statement: Ethical Conduct for Research Involving Humans (TCPS 2); the International Conference on Harmonisation Good Clinical Practice Consolidated Guideline (ICH GCP); Part C, Division 5 of the Food and Drug Regulations; Part 4 of the Natural Health Products Regulations; Part 3 of the Medical Devices Regulations and the provisions of the Ontario Personal Health Information Protection Act (PHIPA 2004) and its applicable regulations. The REB is registered with the U.S. Department of Health & Human Services under the IRB registration number IRB 00000940.

Please do not hesitate to contact us if you have any questions.

Sincerely,

The Office of Human Research Ethics

Note: This correspondence includes an electronic signature (validation and approval via an online system that is compliant with all regulations).

Page 1 of 1

Appendix B: Permission for Reproduction of Scientific Articles

ELSEVIER LICENSE
TERMS AND CONDITIONS

Jan 26, 2023

This Agreement between Paulina Wyszkiewicz ("You") and Elsevier ("Elsevier") consists of your license details and the terms and conditions provided by Elsevier and Copyright Clearance Center.

License Number	5476700043855
License date	Jan 26, 2023
Licensed Content Publisher	Elsevier
Licensed Content Publication	The Lancet
Licensed Content Title	Pathophysiology of airflow limitation in chronic obstructive pulmonary disease
Licensed Content Author	James C Hogg
Licensed Content Date	21–27 August 2004
Licensed Content Volume	364
Licensed Content Issue	9435
Licensed Content Pages	13
Start Page	709
End Page	721
Type of Use	reuse in a thesis/dissertation

Portion	figures/tables/illustrations
Number of figures/tables/illustrations	1
Format	both print and electronic
Are you the author of this Elsevier article?	No
Will you be translating?	No
Title	Longitudinal Computed Tomography Airway Measurements in Ex-Smokers with and without Chronic Obstructive Pulmonary Disease
Institution name	The University of Western Ontario
Expected presentation date	Mar 2023
Portions	Figure 4
Requestor Location	Paulina Wyszkiewicz 1151 Richmond St. N. London, ON N6A 5B7 Canada Attn: Paulina Wyszkiewicz
Publisher Tax ID	GB 494 6272 12
Total	0.00 CAD

Terms and Conditions

INTRODUCTION

1. The publisher for this copyrighted material is Elsevier. By clicking "accept" in connection with completing this licensing transaction, you agree that the following terms and conditions apply to this transaction (along with the Billing and Payment terms and conditions

established by Copyright Clearance Center, Inc. ("CCC"), at the time that you opened your Rightslink account and that are available at any time at http://myaccount.copyright.com).

GENERAL TERMS

2. Elsevier hereby grants you permission to reproduce the aforementioned material subject to the terms and conditions indicated.

3. Acknowledgement: If any part of the material to be used (for example, figures) has appeared in our publication with credit or acknowledgement to another source, permission must also be sought from that source. If such permission is not obtained then that material may not be included in your publication/copies. Suitable acknowledgement to the source must be made, either as a footnote or in a reference list at the end of your publication, as follows:

"Reprinted from Publication title, Vol /edition number, Author(s), Title of article / title of chapter, Pages No., Copyright (Year), with permission from Elsevier [OR APPLICABLE SOCIETY COPYRIGHT OWNER]." Also Lancet special credit - "Reprinted from The Lancet, Vol. number, Author(s), Title of article, Pages No., Copyright (Year), with permission from Elsevier."

4. Reproduction of this material is confined to the purpose and/or media for which permission is hereby given.

5. Altering/Modifying Material: Not Permitted. However figures and illustrations may be altered/adapted minimally to serve your work. Any other abbreviations, additions, deletions and/or any other alterations shall be made only with prior written authorization of Elsevier Ltd. (Please contact Elsevier's permissions helpdesk here). No modifications can be made to any Lancet figures/tables and they must be reproduced in full.

6. If the permission fee for the requested use of our material is waived in this instance, please be advised that your future requests for Elsevier materials may attract a fee.

7. Reservation of Rights: Publisher reserves all rights not specifically granted in the combination of (i) the license details provided by you and accepted in the course of this licensing transaction, (ii) these terms and conditions and (iii) CCC's Billing and Payment terms and conditions.

8. License Contingent Upon Payment: While you may exercise the rights licensed immediately upon issuance of the license at the end of the licensing process for the transaction, provided that you have disclosed complete and accurate details of your proposed use, no license is finally effective unless and until full payment is received from you (either by publisher or by CCC) as provided in CCC's Billing and Payment terms and conditions. If full payment is not received on a timely basis, then any license preliminarily granted shall be deemed automatically revoked and shall be void as if never granted. Further, in the event that you breach any of these terms and conditions or any of CCC's Billing and Payment terms and conditions, the license is automatically revoked and shall be void as if never granted. Use of materials as described in a revoked license, as well as any use of the materials beyond the scope of an unrevoked license, may constitute copyright infringement and publisher reserves the right to take any and all action to protect its copyright in the materials.

9. Warranties: Publisher makes no representations or warranties with respect to the licensed material.

10. Indemnity: You hereby indemnify and agree to hold harmless publisher and CCC, and their respective officers, directors, employees and agents, from and against any and all claims arising out of your use of the licensed material other than as specifically authorized pursuant to this license.

11. No Transfer of License: This license is personal to you and may not be sublicensed, assigned, or transferred by you to any other person without publisher's written permission.

12. No Amendment Except in Writing: This license may not be amended except in a writing signed by both parties (or, in the case of publisher, by CCC on publisher's behalf).

13. Objection to Contrary Terms: Publisher hereby objects to any terms contained in any purchase order, acknowledgment, check endorsement or other writing prepared by you, which terms are inconsistent with these terms and conditions or CCC's Billing and Payment terms and conditions. These terms and conditions, together with CCC's Billing and Payment terms and conditions (which are incorporated herein), comprise the entire agreement between you and publisher (and CCC) concerning this licensing transaction. In the event of any conflict between your obligations established by these terms and conditions and those established by CCC's Billing and Payment terms and conditions, these terms and conditions shall control.

14. Revocation: Elsevier or Copyright Clearance Center may deny the permissions described in this License at their sole discretion, for any reason or no reason, with a full refund payable to you. Notice of such denial will be made using the contact information provided by you. Failure to receive such notice will not alter or invalidate the denial. In no event will Elsevier or Copyright Clearance Center be responsible or liable for any costs, expenses or damage incurred by you as a result of a denial of your permission request, other than a refund of the amount(s) paid by you to Elsevier and/or Copyright Clearance Center for denied permissions.

LIMITED LICENSE

The following terms and conditions apply only to specific license types:

15. **Translation**: This permission is granted for non-exclusive world **English** rights only unless your license was granted for translation rights. If you licensed translation rights you may only translate this content into the languages you requested. A professional translator must perform all translations and reproduce the content word for word preserving the integrity of the article.

16. **Posting licensed content on any Website**: The following terms and conditions apply as follows: Licensing material from an Elsevier journal: All content posted to the web site must maintain the copyright information line on the bottom of each image; A hyper-text must be included to the Homepage of the journal from which you are licensing at http://www.sciencedirect.com/science/journal/xxxxx or the Elsevier homepage for books at http://www.elsevier.com; Central Storage: This license does not include permission for a scanned version of the material to be stored in a central repository such as that provided by Heron/XanEdu.

Licensing material from an Elsevier book: A hyper-text link must be included to the Elsevier homepage at http://www.elsevier.com . All content posted to the web site must maintain the copyright information line on the bottom of each image.

Posting licensed content on Electronic reserve: In addition to the above the following clauses are applicable: The web site must be password-protected and made available only to

bona fide students registered on a relevant course. This permission is granted for 1 year only. You may obtain a new license for future website posting.

17. **For journal authors:** the following clauses are applicable in addition to the above:

Preprints:

A preprint is an author's own write-up of research results and analysis, it has not been peer-reviewed, nor has it had any other value added to it by a publisher (such as formatting, copyright, technical enhancement etc.).

Authors can share their preprints anywhere at any time. Preprints should not be added to or enhanced in any way in order to appear more like, or to substitute for, the final versions of articles however authors can update their preprints on arXiv or RePEc with their Accepted Author Manuscript (see below).

If accepted for publication, we encourage authors to link from the preprint to their formal publication via its DOI. Millions of researchers have access to the formal publications on ScienceDirect, and so links will help users to find, access, cite and use the best available version. Please note that Cell Press, The Lancet and some society-owned have different preprint policies. Information on these policies is available on the journal homepage.

Accepted Author Manuscripts: An accepted author manuscript is the manuscript of an article that has been accepted for publication and which typically includes author-incorporated changes suggested during submission, peer review and editor-author communications.

Authors can share their accepted author manuscript:

- immediately
  - via their non-commercial person homepage or blog
  - by updating a preprint in arXiv or RePEc with the accepted manuscript
  - via their research institute or institutional repository for internal institutional uses or as part of an invitation-only research collaboration work-group
  - directly by providing copies to their students or to research collaborators for their personal use
  - for private scholarly sharing as part of an invitation-only work group on commercial sites with which Elsevier has an agreement
- After the embargo period
  - via non-commercial hosting platforms such as their institutional repository
  - via commercial sites with which Elsevier has an agreement

In all cases accepted manuscripts should:

- link to the formal publication via its DOI
- bear a CC-BY-NC-ND license - this is easy to do
- if aggregated with other manuscripts, for example in a repository or other site, be shared in alignment with our hosting policy not be added to or enhanced in any way to appear more like, or to substitute for, the published journal article.

Published journal article (JPA): A published journal article (PJA) is the definitive final record of published research that appears or will appear in the journal and embodies all value-adding publishing activities including peer review co-ordination, copy-editing, formatting, (if relevant) pagination and online enrichment.

Policies for sharing publishing journal articles differ for subscription and gold open access articles:

Subscription Articles: If you are an author, please share a link to your article rather than the full-text. Millions of researchers have access to the formal publications on ScienceDirect, and so links will help your users to find, access, cite, and use the best available version.

Theses and dissertations which contain embedded PJAs as part of the formal submission can be posted publicly by the awarding institution with DOI links back to the formal publications on ScienceDirect.

If you are affiliated with a library that subscribes to ScienceDirect you have additional private sharing rights for others' research accessed under that agreement. This includes use for classroom teaching and internal training at the institution (including use in course packs and courseware programs), and inclusion of the article for grant funding purposes.

Gold Open Access Articles: May be shared according to the author-selected end-user license and should contain a CrossMark logo, the end user license, and a DOI link to the formal publication on ScienceDirect.

Please refer to Elsevier's posting policy for further information.

18. **For book authors** the following clauses are applicable in addition to the above: Authors are permitted to place a brief summary of their work online only. You are not allowed to download and post the published electronic version of your chapter, nor may you scan the printed edition to create an electronic version. **Posting to a repository:** Authors are permitted to post a summary of their chapter only in their institution's repository.

19. **Thesis/Dissertation**: If your license is for use in a thesis/dissertation your thesis may be submitted to your institution in either print or electronic form. Should your thesis be published commercially, please reapply for permission. These requirements include permission for the Library and Archives of Canada to supply single copies, on demand, of the complete thesis and include permission for Proquest/UMI to supply single copies, on demand, of the complete thesis. Should your thesis be published commercially, please reapply for permission. Theses and dissertations which contain embedded PJAs as part of the formal submission can be posted publicly by the awarding institution with DOI links back to the formal publications on ScienceDirect.

Elsevier Open Access Terms and Conditions

You can publish open access with Elsevier in hundreds of open access journals or in nearly 2000 established subscription journals that support open access publishing. Permitted third party re-use of these open access articles is defined by the author's choice of Creative Commons user license. See our open access license policy for more information.

Terms & Conditions applicable to all Open Access articles published with Elsevier:

Any reuse of the article must not represent the author as endorsing the adaptation of the article nor should the article be modified in such a way as to damage the author's honour or reputation. If any changes have been made, such changes must be clearly indicated.

The author(s) must be appropriately credited and we ask that you include the end user license and a DOI link to the formal publication on ScienceDirect.

If any part of the material to be used (for example, figures) has appeared in our publication with credit or acknowledgement to another source it is the responsibility of the user to ensure their reuse complies with the terms and conditions determined by the rights holder.

Additional Terms & Conditions applicable to each Creative Commons user license:

CC BY: The CC-BY license allows users to copy, to create extracts, abstracts and new works from the Article, to alter and revise the Article and to make commercial use of the Article (including reuse and/or resale of the Article by commercial entities), provided the user gives appropriate credit (with a link to the formal publication through the relevant DOI), provides a link to the license, indicates if changes were made and the licensor is not represented as endorsing the use made of the work. The full details of the license are available at http://creativecommons.org/licenses/by/4.0.

CC BY NC SA: The CC BY-NC-SA license allows users to copy, to create extracts, abstracts and new works from the Article, to alter and revise the Article, provided this is not done for commercial purposes, and that the user gives appropriate credit (with a link to the formal publication through the relevant DOI), provides a link to the license, indicates if changes were made and the licensor is not represented as endorsing the use made of the work. Further, any new works must be made available on the same conditions. The full details of the license are available at http://creativecommons.org/licenses/by-nc-sa/4.0.

CC BY NC ND: The CC BY-NC-ND license allows users to copy and distribute the Article, provided this is not done for commercial purposes and further does not permit distribution of the Article if it is changed or edited in any way, and provided the user gives appropriate credit (with a link to the formal publication through the relevant DOI), provides a link to the license, and that the licensor is not represented as endorsing the use made of the work. The full details of the license are available at http://creativecommons.org/licenses/by-nc-nd/4.0. Any commercial reuse of Open Access articles published with a CC BY NC SA or CC BY NC ND license requires permission from Elsevier and will be subject to a fee.

Commercial reuse includes:

- Associating advertising with the full text of the Article
- Charging fees for document delivery or access
- Article aggregation
- Systematic distribution via e-mail lists or share buttons

Posting or linking by commercial companies for use by customers of those companies.

20. **Other Conditions**:

v1.10

Questions? customercare@copyright.com or +1-855-239-3415 (toll free in the US) or +1-978-646-2777.

JOHN WILEY AND SONS LICENSE
TERMS AND CONDITIONS

Jan 26, 2023

This Agreement between Paulina Wyszkiewicz ("You") and John Wiley and Sons ("John Wiley and Sons") consists of your license details and the terms and conditions provided by John Wiley and Sons and Copyright Clearance Center.

License Number	5476700275190
License date	Jan 26, 2023
Licensed Content Publisher	John Wiley and Sons
Licensed Content Publication	Magnetic Resonance in Medicine
Licensed Content Title	Hyperpolarized 3He diffusion MRI and histology in pulmonary emphysema
Licensed Content Author	Jason C. Woods, Cliff K. Choong, Dmitriy A. Yablonskiy, et al
Licensed Content Date	Oct 20, 2006
Licensed Content Volume	56
Licensed Content Issue	6
Licensed Content Pages	8
Type of use	Dissertation/Thesis

Requestor type	University/Academic
Format	Print and electronic
Portion	Figure/table
Number of figures/tables	1
Will you be translating?	No
Title	Longitudinal Computed Tomography Airway Measurements in Ex-Smokers with and without Chronic Obstructive Pulmonary Disease
Institution name	The University of Western Ontario
Expected presentation date	Mar 2023
Portions	Figure 2
Requestor Location	Paulina Wyszkiewicz 1151 Richmond St. N. London, ON N6A 5B7 Canada Attn: Paulina Wyszkiewicz
Publisher Tax ID	EU826007151
Total	0.00 CAD

Terms and Conditions

TERMS AND CONDITIONS

This copyrighted material is owned by or exclusively licensed to John Wiley & Sons, Inc. or one of its group companies (each a"Wiley Company") or handled on behalf of a society with

which a Wiley Company has exclusive publishing rights in relation to a particular work (collectively "WILEY"). By clicking "accept" in connection with completing this licensing transaction, you agree that the following terms and conditions apply to this transaction (along with the billing and payment terms and conditions established by the Copyright Clearance Center Inc., ("CCC's Billing and Payment terms and conditions"), at the time that you opened your RightsLink account (these are available at any time at http://myaccount.copyright.com).

Terms and Conditions

- The materials you have requested permission to reproduce or reuse (the "Wiley Materials") are protected by copyright.

- You are hereby granted a personal, non-exclusive, non-sub licensable (on a stand-alone basis), non-transferable, worldwide, limited license to reproduce the Wiley Materials for the purpose specified in the licensing process. This license, **and any CONTENT (PDF or image file) purchased as part of your order,** is for a one-time use only and limited to any maximum distribution number specified in the license. The first instance of republication or reuse granted by this license must be completed within two years of the date of the grant of this license (although copies prepared before the end date may be distributed thereafter). The Wiley Materials shall not be used in any other manner or for any other purpose, beyond what is granted in the license. Permission is granted subject to an appropriate acknowledgement given to the author, title of the material/book/journal and the publisher. You shall also duplicate the copyright notice that appears in the Wiley publication in your use of the Wiley Material. Permission is also granted on the understanding that nowhere in the text is a previously published source acknowledged for all or part of this Wiley Material. Any third party content is expressly excluded from this permission.

- With respect to the Wiley Materials, all rights are reserved. Except as expressly granted by the terms of the license, no part of the Wiley Materials may be copied, modified, adapted (except for minor reformatting required by the new Publication), translated, reproduced, transferred or distributed, in any form or by any means, and no derivative works may be made based on the Wiley Materials without the prior permission of the respective copyright owner.**For STM Signatory Publishers clearing permission under the terms of the STM Permissions Guidelines only, the terms of the license are extended to include subsequent editions and for editions in other languages, provided such editions are for the work as a whole in situ and does not involve the separate exploitation of the permitted figures or extracts,** You may not alter, remove or suppress in any manner any copyright, trademark or other notices displayed by the Wiley Materials. You may not license, rent, sell, loan, lease, pledge, offer as security, transfer or assign the Wiley Materials on a stand-alone basis, or any of the rights granted to you hereunder to any other person.

- The Wiley Materials and all of the intellectual property rights therein shall at all times remain the exclusive property of John Wiley & Sons Inc, the Wiley Companies, or their respective licensors, and your interest therein is only that of having possession of and the right to reproduce the Wiley Materials pursuant to Section 2 herein during the continuance of this Agreement. You agree that you own no right, title or interest in or to the Wiley Materials or any of the intellectual property rights therein. You shall have no rights hereunder other than the license as provided for above in Section 2. No right, license or interest to any trademark, trade name, service mark or other branding ("Marks") of WILEY or its licensors is granted hereunder, and you agree that you shall

not assert any such right, license or interest with respect thereto

- NEITHER WILEY NOR ITS LICENSORS MAKES ANY WARRANTY OR REPRESENTATION OF ANY KIND TO YOU OR ANY THIRD PARTY, EXPRESS, IMPLIED OR STATUTORY, WITH RESPECT TO THE MATERIALS OR THE ACCURACY OF ANY INFORMATION CONTAINED IN THE MATERIALS, INCLUDING, WITHOUT LIMITATION, ANY IMPLIED WARRANTY OF MERCHANTABILITY, ACCURACY, SATISFACTORY QUALITY, FITNESS FOR A PARTICULAR PURPOSE, USABILITY, INTEGRATION OR NON-INFRINGEMENT AND ALL SUCH WARRANTIES ARE HEREBY EXCLUDED BY WILEY AND ITS LICENSORS AND WAIVED BY YOU.

- WILEY shall have the right to terminate this Agreement immediately upon breach of this Agreement by you.

- You shall indemnify, defend and hold harmless WILEY, its Licensors and their respective directors, officers, agents and employees, from and against any actual or threatened claims, demands, causes of action or proceedings arising from any breach of this Agreement by you.

- IN NO EVENT SHALL WILEY OR ITS LICENSORS BE LIABLE TO YOU OR ANY OTHER PARTY OR ANY OTHER PERSON OR ENTITY FOR ANY SPECIAL, CONSEQUENTIAL, INCIDENTAL, INDIRECT, EXEMPLARY OR PUNITIVE DAMAGES, HOWEVER CAUSED, ARISING OUT OF OR IN CONNECTION WITH THE DOWNLOADING, PROVISIONING, VIEWING OR USE OF THE MATERIALS REGARDLESS OF THE FORM OF ACTION, WHETHER FOR BREACH OF CONTRACT, BREACH OF WARRANTY, TORT, NEGLIGENCE, INFRINGEMENT OR OTHERWISE (INCLUDING, WITHOUT LIMITATION, DAMAGES BASED ON LOSS OF PROFITS, DATA, FILES, USE, BUSINESS OPPORTUNITY OR CLAIMS OF THIRD PARTIES), AND WHETHER OR NOT THE PARTY HAS BEEN ADVISED OF THE POSSIBILITY OF SUCH DAMAGES. THIS LIMITATION SHALL APPLY NOTWITHSTANDING ANY FAILURE OF ESSENTIAL PURPOSE OF ANY LIMITED REMEDY PROVIDED HEREIN.

- Should any provision of this Agreement be held by a court of competent jurisdiction to be illegal, invalid, or unenforceable, that provision shall be deemed amended to achieve as nearly as possible the same economic effect as the original provision, and the legality, validity and enforceability of the remaining provisions of this Agreement shall not be affected or impaired thereby.

- The failure of either party to enforce any term or condition of this Agreement shall not constitute a waiver of either party's right to enforce each and every term and condition of this Agreement. No breach under this agreement shall be deemed waived or excused by either party unless such waiver or consent is in writing signed by the party granting such waiver or consent. The waiver by or consent of a party to a breach of any provision of this Agreement shall not operate or be construed as a waiver of or consent to any other or subsequent breach by such other party.

- This Agreement may not be assigned (including by operation of law or otherwise) by you without WILEY's prior written consent.

- Any fee required for this permission shall be non-refundable after thirty (30) days from receipt by the CCC.

- These terms and conditions together with CCC's Billing and Payment terms and conditions (which are incorporated herein) form the entire agreement between you and WILEY concerning this licensing transaction and (in the absence of fraud) supersedes all prior agreements and representations of the parties, oral or written. This Agreement may not be amended except in writing signed by both parties. This Agreement shall be binding upon and inure to the benefit of the parties' successors, legal representatives, and authorized assigns.

- In the event of any conflict between your obligations established by these terms and conditions and those established by CCC's Billing and Payment terms and conditions, these terms and conditions shall prevail.

- WILEY expressly reserves all rights not specifically granted in the combination of (i) the license details provided by you and accepted in the course of this licensing transaction, (ii) these terms and conditions and (iii) CCC's Billing and Payment terms and conditions.

- This Agreement will be void if the Type of Use, Format, Circulation, or Requestor Type was misrepresented during the licensing process.

- This Agreement shall be governed by and construed in accordance with the laws of the State of New York, USA, without regards to such state's conflict of law rules. Any legal action, suit or proceeding arising out of or relating to these Terms and Conditions or the breach thereof shall be instituted in a court of competent jurisdiction in New York County in the State of New York in the United States of America and each party hereby consents and submits to the personal jurisdiction of such court, waives any objection to venue in such court and consents to service of process by registered or certified mail, return receipt requested, at the last known address of such party.

WILEY OPEN ACCESS TERMS AND CONDITIONS

Wiley Publishes Open Access Articles in fully Open Access Journals and in Subscription journals offering Online Open. Although most of the fully Open Access journals publish open access articles under the terms of the Creative Commons Attribution (CC BY) License only, the subscription journals and a few of the Open Access Journals offer a choice of Creative Commons Licenses. The license type is clearly identified on the article.

The Creative Commons Attribution License

The Creative Commons Attribution License (CC-BY) allows users to copy, distribute and transmit an article, adapt the article and make commercial use of the article. The CC-BY license permits commercial and non-

Creative Commons Attribution Non-Commercial License

The Creative Commons Attribution Non-Commercial (CC-BY-NC)License permits use, distribution and reproduction in any medium, provided the original work is properly cited and is not used for commercial purposes.(see below)

Creative Commons Attribution-Non-Commercial-NoDerivs License

Appendix C: Curriculum Vitae

Paulina Wyszkiewicz BSc

EDUCATION

2021- Master of Science in Medical Biophysics (Candidate)
Department of Medical Biophysics
Western University, London Canada
Project: Longitudinal Computed Tomography Airway Measurements in Ex-smokers with and without COPD
Co-Supervisors: Dr. Grace Parraga and Dr. Ian Cunningham

2017-2021 Honours Bachelor of Science (Medical Physics)
Department of Physics and Astronomy
Western University, London, Ontario, Canada
Project: Modelling Blood Flow through a Compliant Vessel
Supervisor: Dr. Olga Trichtchenko

ACADEMIC POSITIONS AND EMPLOYMENT

2021- **Western University**
Graduate Research Fellowship
Department of Medical Biophysics

2021 **Robarts Research Institute**
Summer Student Research Trainee

2020-2021 **Western University French Immersion School Trois-Pistoles**
French Virtual Learning Assistant

2020 **Quantum Institute at the University of Sherbrooke**
Summer Research Intern

2019-2020 **Western University**
Undergraduate Student Researcher
Department of Physics and Astronomy

2019 **Western University**
Laboratory and Research Assistant
Department of Physics and Astronomy

2015-2019 **London Music Conservatory**
Piano and Violin Instructor

2015-2017 **Kumon Learning Centre**
Math and Reading Instructor

HONOURS, AWARDS AND RECOGNITIONS

2023 **CTS Research Poster Competition**
Top 30 abstracts submitted by Canadian trainees to the ATS Annual Meeting are selected to compete in a poster competition
National

2022 **Western Graduate Research Scholarship, Western University**
Awarded to a full time graduate student for stipend support who had maintained an average of 80% or more
Institutional
$5,000

2021 **Western Graduate Research Scholarship, Western University**
Awarded to a full time graduate student for stipend support who had maintained an average of 80% or more
Institutional
$5,000

2020 **Laurene Paterson Estate Scholarship, Western University**
Awarded annually to full-time undergraduate students in any year in the Faculty of Science who have maintained a minimum 80% average
Institutional
$2,000

2020 **Dean's Honour List, Western University**
Institutional

2017 **Frank Wierzbicki Bursary**
Institutional
$250

2017 **Western Scholarship of Excellence, Western University**
Awarded to an incoming student based on outstanding academic achievement with an admission average of 90% or more
Institutional
$2,000

2016 **Western's Initiative for Scholarly Excellence, Western University**
Awarded to high achieving students to take one course tuition free at Western University concurrently with their secondary school studies
Institutional

POST-GRADUATE EDUCATION DEVELOPMENT

2022-2023 **Graduate Academic Mentor**
Academic Mentorship Program
Graduate Student: Samantha Flood MSc Candidate

2022-2023	**Graduate Student Mentor** *Undergraduate Student:* Madeline Ico BSc Candidate *Project:* "CT Pulmonary Vascular Measurements in Ex-smokers with and without COPD and Healthy Elderly Volunteers"
2022-2023	**Graduate Student Mentor** *Undergraduate Student:* Vedanth Desaigoudar BSc Candidate *Project:* "Ex-smokers with and without COPD: Investigating CT Pulmonary Vascular and Airway Measurements"

LEADERSHIP

2021-2022	**World Lung Day Awareness Event, Western University** *Funded by Healthy Lungs for Life from the European Lung Foundation* Event Director
2020-2021	**Physics and Astronomy Student Association, Western University** General Vice-President
2019-2021	**Polish Student's Union, Western University** Vice-President of Cultural Affairs
2017-2018	**Polish Student's Union, Western University** First Year Representative

COMMUNITY AND VOLUNTEER ACTIVITIES

2021-2022	**St. John's Hospitality Services** Volunteer
2019	**Boys and Girls Club of London** Volunteer
2019	**ReForest London** Volunteer
2018	**Centre de Santé et des Services Sociaux des Basques** Volunteer

COMMITTEES AND PROFESSIONAL ACTIVITIES

2022-	**Western Polish Graduate Student Association, Western University** Member
2021-	**Deep Learning Club, Western University** Member

2021-2022	**Medical Biophysics CAMPEP Student Club, Western University** Member
2021-	**Medical Biophysics Teaching Interest Group, Western University** Member
2020-2021	**Physics Undergraduate Conference Committee, Western University** Member: Leader and Organizer
2020	**Canadian Undergraduate Physics Conference Committee** Member
2019-2020	**Physics Undergraduate Conference Committee, Western University** Member
2018-2021	**Physics and Astronomy Student Association, Western University** Member
2017-2021	**Polish Student's Union, Western University** Member

PUBLICATIONS AND PRESENTATIONS

A Peer-Reviewed Journal Manuscripts

Published (1)

1. M Sharma, **PV Wyszkiewicz**, V Desaigoudar, D Capaldi, F Guo and G Parraga. Quantification of Pulmonary Functional MRI: State-of-the-Art and Emerging Image Processing Methods and Measurements. Physics in Medicine & Biology. 2022.

Submitted (1)

1. **PV Wyszkiewicz**, M Sharma, V Desaigoudar, IA Cunningham, DG McCormack, M Abdelrazek, M Kirby and G Parraga. Reduced Total Airway Count and Airway Wall Tapering after Three-year in Ex-smokers. *Submitted to Journal of Chronic Obstructive Pulmonary Disease on February 3, 2023*.

B Published Conference Abstracts

Submitted (2)

1. **PV Wyszkiewicz**, M Sharma, HK Kooner, DG McCormack, M Kirby and G Parraga. Terminal Airspace Enlargement Measured Using Pulmonary Functional MRI Predicts CT Airway Loss in COPD. Annual International Society of Magnetic Resonance in Medicine Scientific Meeting 2023, Toronto, Canada. June 3-8, 2023.
2. M Sharma, **PV Wyszkiewicz**, HK Kooner, MJ McIntosh, DG McCormack and G Parraga. All-cause Mortality Predicted Using Pulmonary Functional MRI. Annual International Society of Magnetic Resonance in Medicine Scientific Meeting 2023, Toronto, Canada. June 3-8, 2023.

Accepted (12)

1. **PV Wyszkiewicz**, M Sharma, V Desaigoudar, DG McCormack, M Kirby and G Parraga. Progressive Airway Wall Thinning and Loss of Total Airway Count after Three-Years in COPD. American Thoracic Society Annual Scientific Meeting. Washington, DC. May 19-24, 2023. *Accepted Oral Presentation.*
2. M Sharma, **PV Wyszkiewicz**, MJ McIntosh, HK Kooner, AM Matheson, DG McCormack and G Parraga. MRI and CT Measurements Uniquely Explain All-cause Mortality in Ex-smokers with and without COPD. American Thoracic Society Annual Scientific Meeting. Washington, DC. May 19-24, 2023. *Accepted Oral Presentation.*
3. HK Kooner, M Faran, MJ McIntosh, AM Matheson, **PV Wyszkiewicz**, I Dhaliwal, M Abdelrazek, JM Nicholson, and G Parraga. Sex Differences in CT Airway Measurements and their Relationship to Post-Acute COVID-19 Syndrome. American Thoracic Society Annual Scientific Meeting. Washington, DC. May 19-24, 2023. *Accepted Poster Presentation.*
4. **PV Wyszkiewicz**, M Sharma, V Desaigoudar, DG McCormack, M Kirby and G Parraga. Progressive Airway Wall Thinning and Loss of Total Airway Count after Three-Years in COPD. Imaging Network Ontario Annual Symposium. London, ON. March 23-24, 2023.
5. M Sharma, **PV Wyszkiewicz**, MJ McIntosh, HK Kooner, AM Matheson, DG McCormack and G Parraga. CT and MRI Measurements Uniquely Explain All-cause Mortality in Ex-smokers. Imaging Network Ontario Annual Symposium. London, ON. March 23-24, 2023.
6. V Desaigoudar, **PV Wyszkiewicz**, AM Matheson, M Sharma, MJ McIntosh, HK Kooner, DG McCormack, M Kirby and G Parraga. Pulmonary Small Vessel Worsening in Ex-smokers with COPD. Imaging Network Ontario Annual Symposium. London, ON. March 23-24, 2023.
7. **PV Wyszkiewicz**, M Sharma, DG McCormack, IA Cunningham and G Parraga. CT Pulmonary Airways in Chronic Obstructive Pulmonary Disease: Longitudinal Worsening in the TINCan Cohort Study. Robarts Research Retreat. London ON, Canada. June 16, 2022. *Accepted Poster Presentation.*
8. M Sharma, MJ McIntosh, HK Kooner, AM Matheson, **PV Wyszkiewicz**, DG McCormack, and G Parraga. Texture Analysis and Machine Learning of Hyperpolarized 3He MRI Ventilation Predicts Quality-of-life Worsening in Ex-smokers with and without COPD. Robarts Research Retreat. London ON, Canada. June 16 2022. *Accepted Poster Presentation.*
9. HK Kooner, MJ McIntosh, AM Matheson, M Sharma, **PV Wyszkiewicz**, I Dhaliwal, M Abdelrazek, M Nicholson, and G Parraga. 129Xe MRI Ventilation Defects in People with Post-Acute COVID-19 Syndrome. Robarts Research Retreat. London ON, Canada. June 16, 2022. *Accepted Oral Presentation.*
10. **PV Wyszkiewicz**, M Sharma, DG McCormack, IA Cunningham and G Parraga. CT Pulmonary Airways in Chronic Obstructive Pulmonary Disease: Longitudinal Worsening in the TINCan Cohort Study. London Imaging Discovery Day. London ON, Canada. June 9, 2022. *Accepted Oral Presentation.*
11. M Sharma, MJ McIntosh, HK Kooner, AM Matheson, **PV Wyszkiewicz**, DG McCormack, and G Parraga. Texture Analysis and Machine Learning of Hyperpolarized 3He MRI Ventilation Predicts Quality-of-life Worsening in Ex-smokers with and without COPD. London Imaging Discovery Day. London ON, Canada. June 9, 2022. *Accepted Oral Presentation.*
12. HK Kooner, MJ McIntosh, AM Matheson, M Sharma, **PV Wyszkiewicz**, I Dhaliwal, M Abdelrazek, M Nicholson, and G Parraga. 129Xe MRI Ventilation Defects in People with Post-Acute COVID-19 Syndrome. London Imaging Discovery Day. London ON, Canada. June 9, 2022. *Accepted Oral Presentation.*

C **Proffered Oral Presentations (5)** *presenter

1. HK Kooner, MJ McIntosh, AM Matheson, M Sharma, **PV Wyszkiewicz**, I Dhaliwal, M Abdelrazek, M Nicholson, and G Parraga. 129Xe MRI Ventilation Defects in People with Post-Acute COVID-19 Syndrome. Robarts Research Retreat. London ON, Canada. June 16, 2022.
2. **PV Wyszkiewicz***, M Sharma, DG McCormack, IA Cunningham and G Parraga. CT Pulmonary Airways in Chronic Obstructive Pulmonary Disease: Longitudinal Worsening in the TINCan Cohort Study. London Imaging Discovery Day. London ON, Canada. June 9, 2022.
3. M Sharma, MJ McIntosh, HK Kooner, AM Matheson, **PV Wyszkiewicz**, DG McCormack, and G Parraga. Texture Analysis and Machine Learning of Hyperpolarized 3He MRI Ventilation Predicts Quality-of-life Worsening in Ex-smokers with and without COPD. London Imaging Discovery Day. London ON, Canada. June 9, 2022.
4. HK Kooner, MJ McIntosh, AM Matheson, M Sharma, **PV Wyszkiewicz**, I Dhaliwal, M Abdelrazek, M Nicholson, and G Parraga. 129Xe MRI Ventilation Defects in People with Post-Acute COVID-19 Syndrome. London Imaging Discovery Day. London ON, Canada. June 9, 2022.
5. **PV Wyszkiewicz*** and O Trichtchenko. Modelling Blood Flow through a Vessel. Western University Physics Honours Thesis Presentations, Virtual. April 27, 2021.

D Proffered Poster Presentations (4) *presenter

1. **PV Wyszkiewicz***, M Sharma, V Desaigoudar, DG McCormack, M Kirby and G Parraga. Progressive Airway Wall Thinning and Loss of Total Airway Count after Three-Years in COPD. 10th Annual Canadian Thoracic Society Poster Competition at American Thoracic Society Annual Scientific Meeting. Washington, DC. May 20, 2023.
2. **PV Wyszkiewicz***, M Sharma, DG McCormack, IA Cunningham and G Parraga. CT Pulmonary Airways in Chronic Obstructive Pulmonary Disease: Longitudinal Worsening in the TINCan Cohort Study. Robarts Research Retreat. London ON, Canada. June 16, 2022.
3. M Sharma, MJ McIntosh, HK Kooner, AM Matheson, **PV Wyszkiewicz**, DG McCormack, and G Parraga. Texture Analysis and Machine Learning of Hyperpolarized 3He MRI Ventilation Predicts Quality-of-life Worsening in Ex-smokers with and without COPD. Robarts Research Retreat. London ON, Canada. June 16 2022.
4. **PV Wyszkiewicz*** and L Goncharova. Multichannel Analyzer Senior Laboratory Project. Physics Undergraduate Conference, Virtual. March 11, 2021.

PROFESSIONAL SOCIETIES

2021-	American Thoracic Society (ATS) *Trainee Member*
2021-	Canadian Thoracic Society (CTS) *Student Member*
2021-	European Respiratory Society (ERS) *Student Member*
2021-	International Society for Magnetic Resonance in Medicine (ISMRM) *Trainee Member*